CrossMark

ORIGINAL RESEARCH PAPER

Damage classification and derivation of damage probability matrices from L'Aquila (2009) post-earthquake survey data

A. Rosti[1,2] · **M. Rota**[3] ⬦ · **A. Penna**[2,3]

Abstract Post-earthquake damage data represent an invaluable source of information for the seismic vulnerability assessment of the exposed building stock, as they are a direct evidence of the actual buildings' performance under real seismic events. This paper exploits a robust and homogeneous database of damage data collected after the 2009 L'Aquila (Italy) earthquake, to derive damage probability matrices for several building typologies representative of the Italian building stock. To this aim, the first part of the work investigates several issues related to the definition of damage to be associated with each inspected building. Different approaches and damage conversion rules are applied, pointing out advantages and weaknesses of each one. Considering the widespread seismic damage observed on masonry infill panels and partitions of reinforced concrete constructions, the impact of this type of non-structural damage on empirical damage and functional loss distributions is explored. The second part of the study proposes different possible interpretations of the repartition of the observed damage in the different damage levels, showing in some cases a bimodal trend. Two novel hybrid procedures are outlined and compared with the classical binomial approach for predicting the subdivision of damage in the different levels. The application of the proposed methodologies to the different building typologies allows the selection, for each one, of the method providing the best fit to empirical results. The parameters required for the application of the optimal approach are reported in the paper, so that results can be used for forecasting the expected seismic damage in sites with similar seismic hazard and exposed buildings.

Keywords Empirical seismic vulnerability · Damage probability matrices · Damage and usability assessment · Pre-existing damage · Binomial distribution

✉ M. Rota
  maria.rota@eucentre.it

[1] ROSE Programme, UME School, IUSS, Via Ferrata 1, 27100 Pavia, Italy

[2] Department of Civil Engineering and Architecture, University of Pavia, Via Ferrata 3, 27100 Pavia, Italy

[3] EUCENTRE Foundation, Via Ferrata 1, 27100 Pavia, Italy

🍕 Springer

1 Introduction

On the 6th of April 2009, a destructive earthquake struck the city of L'Aquila and the surrounding region in Central Italy, causing extensive damage, human casualties and homeless people. In the past, the Aterno valley has been frequently hit by earthquakes, some of them with local origin. The city of L'Aquila, founded in the late XIII century, suffered macroseismic intensities exceeding degree VII (MCS) more than five times, with peaks of IX due to the 1349, 1461 and 1703 seismic events. In addition, less devastating but still frequent earthquakes struck the city (Galli et al. 2009; Stucchi et al. 2009).

The macroseismic surveys, carried out in the aftermath of the 2009 seismic event, identified the most damaged area, extending in the NW–SE direction from the epicentral zone. Sixteen localities were assigned macroseismic intensity at least equal to degree VIII (MCS). Six sites reported intensity degree IX or even higher, among which Castelnuovo and Onna (IX–X MCS) were the most severely damaged villages (Galli et al. 2009). The majority of severe damages and structural collapses concerned masonry buildings and, in particular, constructions with poor-quality masonry, lacking construction details and with significant irregularities (e.g. Carocci and Lagomarsino 2009; Augenti and Parisi 2010; D'Ayala and Paganoni 2011; Rossetto et al. 2011). The poor seismic performance of unreinforced masonry buildings was mainly ascribed to the poor quality (weak mortar) and texture (rubble or poorly squared stonework) of masonry and to the lack of connection of the masonry leaves, which in some cases disaggregated under the seismic action. Although several connecting devices, most of them dating back to the reconstruction process following the 1703 earthquake, were observed along the buildings' height, out-of-plane collapses were not prevented due to the absence of proper connections between the façade and the orthogonal walls (Carocci and Lagomarsino 2009). In other cases, widespread damage was driven by bad maintenance and/or poor quality of wooden structures, constituting flexible diaphragms and roofs, and their lack of connection with the vertical bearing structure. Damage associated with in-plane mechanisms was also observed, particularly in buildings where local out-of-plane mechanisms were prevented by good connections between vertical walls and horizontal structures, possibly with the presence of transversal tie-rods. However, there were also several cases of masonry constructions exhibiting a satisfactory seismic performance, thanks to the good quality of materials, regular distribution of the openings and good construction details (Augenti and Parisi 2010).

Reinforced concrete (RC) buildings showed low percentages of structural damage, with few cases only of total collapse or severe damage observed in the L'Aquila city centre (i.e. the University dormitory and the Duca degli Abruzzi hotel). By contrast, non-structural damage was extensive, with varying levels of damage to infill masonry panels and internal partitions. In some cases, despite buildings being repairable, the extent of damage impeded their immediate re-occupancy. In other cases, the collapse of masonry infills and cladding caused heavy socio-economic consequences, from human fatalities to functional loss (e.g. D'Ayala and Dolce 2011; Rossetto et al. 2011; Braga et al. 2011; Ricci et al. 2011).

The widespread damage caused by the L'Aquila seismic event on different construction types recalled the need for setting reliable tools for the seismic vulnerability assessment of the exposed building stock. Different approaches, primarily classified based on data nature, are available in the literature. Among these, empirical methods, statistically processing damage data collected during post-earthquake field surveys, represent a sort of in situ test of the seismic vulnerability of existing buildings. With proper treatment of the several sources of uncertainty and accurate processing, post-earthquake damage data can be also

used to validate and/or calibrate analytical models (e.g. Molina et al. 2014; De Luca et al. 2015).

The seismic vulnerability of buildings can be quantified by means of damage probability matrices (DPMs), providing the distribution of damage in different levels for a preselected ground motion intensity level, or by empirical fragility curves, representing continuous relationships between the observed seismic damage and the ground motion intensity measure (e.g. Rossetto and Elnashai 2003; Rota et al. 2008; Hancilar et al. 2013; Hsieh et al. 2013; Rossetto et al. 2013; Pomonis et al. 2014; Kouris 2016; Buratti et al. 2017).

Past works focused on the seismic input characterisation, by explicitly modelling the spatial ground motion variability (Yazgan 2015) and assessing its impact on empirical fragility curves (Ioannou et al. 2015) and by considering a refined ground motion characterisation (Hsieh et al. 2013). By contrast, very few studies focused on the definition of damage, widely exploring its multifaceted aspects and their implications on results (e.g. Di Pasquale and Goretti 2001; Lagomarsino et al. 2015).

The expected performance of a building is generally modelled on discrete damage scales, with damage states that need to be unambiguously defined and associated with the damage descriptions provided by the survey forms. The overall damage of a building depends on both the distribution and the severity of damage to the different building components and is obtained from the highest or average damage of the different parts of the structure. This is carried out based on a series of assumptions, with little care on the impact of each choice on the results, as well as on the selection of building components for the definition of a unique global damage.

Given that post-earthquake damage assessment is typically oriented to the building's usability classification, the suitability of the adopted damage scale could be tested against the functional loss of buildings. In this case, non-structural damage should be included in the definition of damage levels, as past earthquakes worldwide demonstrated that failure of non-structural elements can imply consistent economic loss to the building and disruption of its functionality, even if the main load-bearing structure is only slightly damaged (e.g. Braga et al. 2011; Miranda et al. 2012; Vicente et al. 2012; Filiatrault and Sullivan 2014). Among non-structural damages, damage to infill masonry panels, typically used in RC buildings, is particularly relevant, as it can have serious effects on both human safety and building functionality.

The interpretation of empirical damage data can be often tricky and controversial, due to several uncertainties in the acquired data, mostly related to the need of inspecting many buildings in a limited time span, to non-uniformly skilled surveyors and to the issue of completeness of field surveys (e.g. Rossetto et al. 2013). Another issue may be represented by pre-existing damage, often due to bad maintenance conditions. Although more recent survey forms allow to indicate the presence of some level of pre-existing damage, this information is not easy to be quantified, particularly when affecting the lower levels of damage.

Starting from these considerations, this paper takes advantage of the L'Aquila post-earthquake damage data (described in Sect. 2), to explore different definitions of damage, with reference to residential building typologies. Different procedures are adopted to derive empirical damage distributions and their impact on damage distribution is assessed (Sect. 3). Usability distributions conditioned on the level of damage are then derived by considering two damage definitions, primarily differing for the inclusion of non-structural damage on masonry infills and partitions, which is significant in case of reinforced concrete buildings (Sect. 4). The observation of a bimodal trend in the empirical damage distributions suggested the development of two hybrid procedures, providing a suitable model

for the derivation of consistent damage probability matrices (Sect. 5). The feasibility of both procedures is demonstrated with reference to a case study. The accuracy of each approach is then compared to the classical binomial model, in terms of a synthetic error parameter, allowing the identification of the procedure providing, for each building typology, the best fit between observations and predictions. Final remarks and conclusions are lastly discussed in Sect. 6.

2 The L'Aquila damage database

In the immediate aftermath of the main shock, a widespread damage and usability assessment was launched. Buildings' inspections were carried out by using the first level form for post-earthquake damage assessment, short-term countermeasures and usability assessment of ordinary buildings, called AeDES form (Baggio et al. 2007). This form, which is an improved version of the form used in the 1997 Umbria-Marche and 1998 Pollino seismic events, is oriented to survey typological, damage and usability characteristics of residential buildings in the emergency phase following a seismic event.

The L'Aquila damage database obtained from this assessment counted more than 73,000 survey forms of buildings distributed in 129 municipalities of the Abruzzi region. The inspections of ordinary buildings were carried out for all the buildings located in settlements where macroseismic surveys assigned (MCS) macroseismic intensity higher than VI (Galli et al. 2009). In all the other cases, buildings were inspected only if requested by the owner (Dolce and Goretti 2015), with the consequence that the survey is not complete and it tends to be limited to buildings with some level of damage. If not properly accounted for, the incompleteness of post-earthquake surveys at a given locality can lead to large under-coverage errors, with a consequent bias in the resulting damage estimates (Rossetto et al. 2013). Based on these considerations, a complete damage dataset was identified, including only data regarding buildings in localities that were completely surveyed (i.e. all buildings). These were selected according to the following criteria: in addition to localities with associated macroseismic intensity higher than VI, all the sites with a threshold of completeness exceeding 90% (i.e. in which at least 90% of the existing buildings were inspected, according to Census data 2001) were considered to be completely surveyed, similarly to other existing works (e.g. Sabetta et al. 1998; Goretti and Di Pasquale 2004; Rota et al. 2008). Based on these assumptions, the complete dataset reduced to almost 51,000 buildings.

The AeDES survey form consists of different sections, collecting metrical, typological and damage data of each inspected building. A process of interpretation was necessary to consistently group damage data into building typologies and levels of damage. Additionally, a measure of the ground motion shaking was assigned to each inspected building.

2.1 Identification of building typologies

The L'Aquila and, more generally, the Abruzzi urban fabric shows a very heterogeneous residential building stock, with different structural typologies. This heterogeneity is mainly ascribed to the presence of buildings of various age, architectural styles and construction materials. Masonry is the predominant building material in the affected area, where local rubble stone, roughly squared stone blocks mixed with bricks, sometimes in regular courses, brick masonry and dressed stone blocks are commonly adopted. Several cases of *a*

sacco masonry were also found, consisting of two external wythes of dressed or partially dressed stones with an inner core filled by rubble material. The original horizontal structural systems typically consist of wooden diaphragms and roofs, although masonry vaults at the first floor, combined with timber horizontal structures at the upper levels, are also common. In some masonry buildings, reinforced concrete slabs and roof replaced wooden diaphragms and roof. Also, mixed structures, with both masonry and reinforced concrete elements, resulting from modifications throughout the years, can be observed (Carocci and Lagomarsino 2009; D'Ayala and Paganoni 2011; Rossetto et al. 2011). This huge variety of construction ages and materials implies a remarkable variety of existing buildings with different characteristics and construction details, not only within the Abruzzi region but even within the same town.

The statistical analysis of the complete and usable post-earthquake damage data confirms the predominance of masonry with respect to other construction materials, representing about 69% of the existing building stock (Fig. 1). Most masonry buildings consist of irregular texture or poor-quality masonry ("IMA" in Fig. 1), although constructions with regular layout and good-quality masonry ("RMA") are also common.

The aim of classifying constructions according to a predefined taxonomy is to collect elements with a similar expected seismic performance. In this work, buildings were subdivided into twenty-three structural typologies (Table 1), based on the RISK-UE (2004) typological classification, suitably adapted by Rota et al. (2008). Buildings were first classified according to the type of vertical bearing structure, i.e. masonry, reinforced concrete, mixed (i.e. masonry and reinforced concrete) and steel. With the only exception of steel buildings, additional sub-typologies were then introduced to capture possible differences within the main class. In case of mixed structures, two sub-categories were introduced, considering the number of storeys above the ground level. Reinforced concrete buildings were further subdivided depending on the number of storeys and seismic design criteria at the time of construction. To this aim, the age of construction of the building was compared with the year of seismic classification of the municipality, to establish if a building was designed and built according to seismic prescriptions or not. Buildings were considered to be seismically designed when constructed after 1975, in a municipality already classified as "seismic" at the time of construction. The seismic performance of masonry buildings is also affected by quality of construction and details. Hence, additional
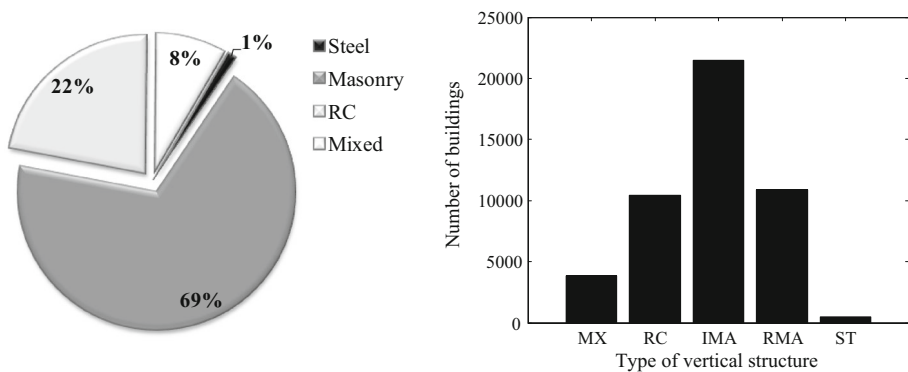

Fig. 1 Subdivision of data based on the type of vertical structure: "MX" indicates mixed masonry and RC buildings, "IMA" and "RMA" are irregular texture or poor-quality masonry buildings and regular layout and good-quality masonry buildings, respectively; "ST" is for steel buildings

Table 1 Identified building typologies and corresponding number of buildings (into brackets)

	Mixed	Reinforced Concrete		Irregular texture or poor-quality masonry				Regular texture and good-quality masonry				Steel
		Seismic design	No seismic design	Flexible diaphragms		Rigid diaphragms		Flexible diaphragms		Rigid diaphragms		
				with CD[c]	w/o CD[c]	with CD[c]	w/o CD[c]	with CD[c]	w/o CD[c]	with CD[c]	w/o CD[c]	
L[a]	MX1 (2186)	RC1 (6659)	RC2 (966)	IMA1 (1922)	IMA2 (7227)	IMA3 (1162)	IMA4 (2430)	RMA1 (1039)	RMA2 (1851)	RMA3 (3035)	RMA4 (992)	ST (492)
M/H[b]	MX2 (1685)	RC3 (2261)	RC4 (570)	IMA5 (1665)	IMA6 (4276)	IMA7 (854)	IMA8 (1183)	RMA5 (497)	RMA6 (602)	RMA7 (2127)	RMA8 (487)	

No of buildings	<1000	> 1000 < 2000	> 2000 < 3000	> 3000 < 4000	> 4000 < 5000	> 5000

[a]Low-rise: 1–2 storeys for mixed and masonry building typologies; 1–3 storeys for reinforced concrete building typologies

[b]Mid-/High-rise: > 2 storeys for mixed and masonry building typologies; > 3 storeys for reinforced concrete building typologies

[c]Connecting devices: tie-rods and/or tie-beams

refinements were considered, such as the layout and quality of masonry (i.e. buildings with irregular layout or poor-quality masonry and buildings with regular layout and good-quality masonry), the in-plane flexibility of the horizontal structure (i.e. rigid or flexible), the number of storeys and the presence or absence of connecting devices (e.g. tie-rods and tie-beams).

2.2 Ground motion characterisation

Different ground motion intensity measures, such as for example peak ground motion parameters and macroseismic intensity scales, can be adopted for representing the severity of ground motion for the derivation of empirical damage probability matrices. In this work, the peak ground acceleration (PGA) was selected, although this ground motion intensity measure does not seem to generally provide a good correlation with damage. However, being very often considered by European seismic building codes for loads definition and given its extensive use in seismic hazard maps, it has been broadly adopted for the seismic vulnerability assessment (e.g. Sabetta et al. 1998; Rossetto and Elnashai 2003; Rota et al. 2008; Liel and Lynch 2009; Del Gaudio et al. 2017).

Isoseismic units were defined at the municipality level, where a unique PGA value was estimated via an up-to-date ground motion prediction equation (GMPE, Bindi et al. 2014a, b). For consistency with the selected prediction equation, the main characteristics of the L'Aquila seismic event (e.g. earthquake location, magnitude and style-of-faulting) were retrieved from the RESORCE database (Akkar et al. 2014), on which the GMPE is based. Although the selected GMPE allows to account for local site conditions, in this study the peak ground acceleration was estimated on equivalent rock, since the soil type at each affected building is unknown. Given that the Italian seismic hazard map is expressed in terms of PGA on sites with $V_{s,30} > 800$ m/s, this choice could allow to derive fragility curves to be consistently used together with seismic hazard estimates for seismic risk

scenarios (e.g. Rota et al. 2011). Figure 2 (left) shows the municipalities that were completely surveyed (solid hatch), in the Abruzzi region, with the grey scale indicating the corresponding PGA values. The right part depicts instead the number of inspected buildings for each PGA interval. The considerable number of buildings in the PGA range of 0.25–0.30 g primarily derives from constructions sited in the municipality of L'Aquila.

2.3 Observed damage

The AeDES survey form classifies the damage observed during the survey on different building components in terms of both severity and extent (Table 2). Focusing on the severity of the observed damage, the form grades three levels of damage, that is slight damage (D1), medium-severe damage (D2–D3) and very heavy damage (D4–D5), in addition to the case of null damage.

Figure 3 shows the proportion of damaged buildings of the considered dataset, according to the observed damage level and extent on four different building components, in accordance with the survey form. A significant percentage of damage level D1 is observed for an extent lower than 1/3, independently of the building component. In case of damage levels D2–D3 and D4–D5, the most likely cases correspond to extent of < 1/3 and > 2/3, respectively. Figure 4 shows the distribution of damaged buildings, according to the information on the observed damage reported by the forms, conditioned on the type of vertical structure and building component. It can be noted that buildings with irregular texture or poor-quality masonry (IMA) exhibit the highest frequency of occurrence of damage levels D2–D3 and D4–D5, with respect to other structural typologies. Both Figs. 3 and 4 refer to the damage description of the survey form and, in case of multiple choice, to the most severe case.

With reference to the structural typologies defined in this work, Fig. 5a shows the observed frequency of the different levels of damage for reinforced concrete buildings, on vertical structure (left) and masonry infills/partitions (right). In the figures, white corresponds to DS0, light grey to DS1, dark grey to DS2–DS3 and black to DS4–DS5. As expected, the least damaged building typology corresponds to low-rise reinforced concrete buildings with seismic design (i.e. RC1), whereas building typology RC4, including medium-/high-rise RC buildings not following any seismic prescription, appears to be the most vulnerable. The severity of damage increases with the number of storeys, although high frequencies of null damage are observed on the vertical structure, in accordance with
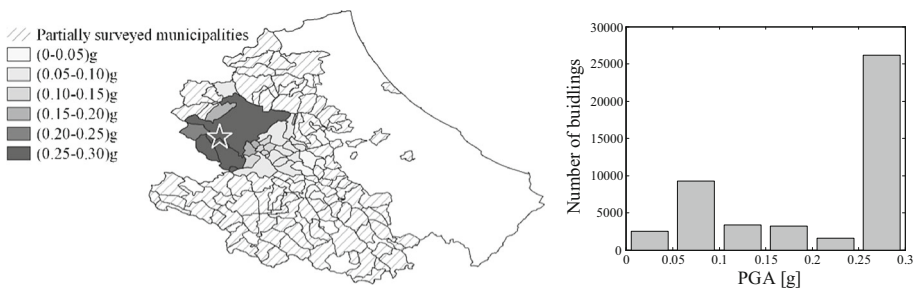

Fig. 2 Identification of the municipalities that were partially (dashed area) and completely (solid hatch) surveyed within the Abruzzi region, with the grey scale indicating the PGA range (left); number of inspected buildings (right) per PGA interval

Table 2 AeDES damage grades and extent for different structural components

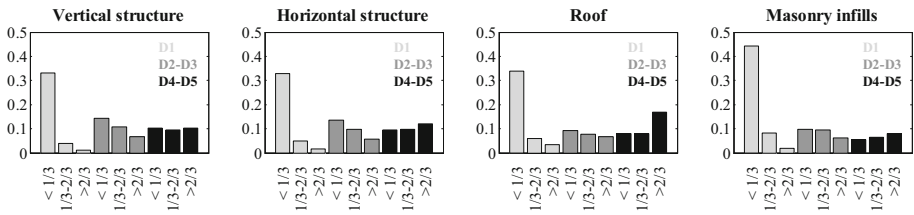| Level—extent	Damage									Null
	D4–D5 very heavy			D2–D3 medium-severe			D1 slight			
Structural component	> 2/3	1/3–2/3	< 1/3	> 2/3	1/3–2/3	< 1/3	> 2/3	1/3–2/3	< 1/3	
1. Vertical structure	❑	❑	❑	❑	❑	❑	❑	❑	❑	❍
2. Horizontal structure	❑	❑	❑	❑	❑	❑	❑	❑	❑	❍
3. Stairs	❑	❑	❑	❑	❑	❑	❑	❑	❑	❍
4. Roof	❑	❑	❑	❑	❑	❑	❑	❑	❑	❍
5. Masonry infills—partitions	❑	❑	❑	❑	❑	❑	❑	❑	❑	❍

Fig. 3 Observed frequency of the different damage levels and extents on different building components
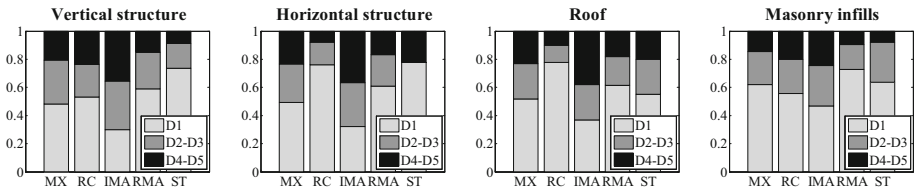

Fig. 4 Observed frequency of each damage level, for different building components and types of vertical structure
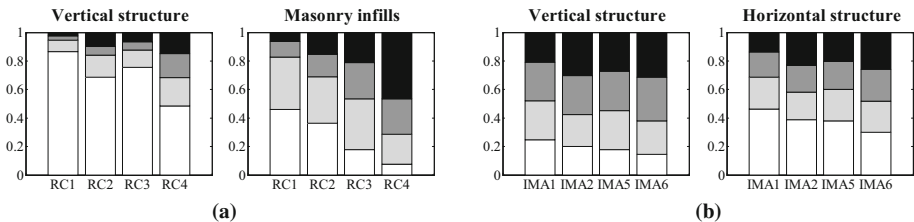

Fig. 5 Observed frequency of the different damage levels for selected structural typologies and for different building components: **a** RC building typologies; **b** irregular texture or poor-quality masonry. White corresponds to DS0, light grey to DS1, dark grey to DS2–DS3 and black to DS4–DS5

reconnaissance surveys carried out in the aftermath of the seismic event (e.g. Braga et al. 2011; Ricci et al. 2011). Differently, significant damage is observed on masonry infills and partitions.

Figure 5b depicts the frequency of damage levels observed on the vertical (left) and horizontal (right) structures of four masonry building typologies, all with irregular layout or poor-quality masonry and flexible diaphragms. The four selected building typologies differ for the number of storeys and presence of connecting devices. Focusing on damage on the vertical structure, the comparison of building typologies with equal number of storeys (i.e. IMA1 and IMA2; IMA5 and IMA6) shows higher seismic vulnerability if tie-rods and tie-beams are absent. The comparison of typologies IMA1 with IMA5 and IMA2 with IMA6 seems to confirm that the number of storeys is another key parameter affecting the seismic response. Based on these considerations, building typology IMA1 and IMA6 turn out to be the least and the most vulnerable typologies, respectively. Similar considerations apply to damage to the horizontal structure.

3 Alternative damage definitions

3.1 Approaches for the definition of buildings' damage levels

Empirical vulnerability studies require the association of a univocal damage state with each inspected construction, starting from the information on observed damage reported in the survey form and establishing a suitable relation with the selected damage scale. As discussed in Sect. 2.3, the AeDES damage description is articulated into three levels plus the case of null damage, representing condensed damage levels of the EMS98 macroseismic scale (Grünthal 1998). Damage states are identified by quantitative measures of different types of damage, visually detected on structural and non-structural components, and are primarily oriented to the safety assessment. The different approaches available in the literature for assigning a unique damage level to each inspected building can be classified into two main categories, based either on average damage or maximum damage.

The first class of approaches condenses damage levels of the different building components into a unique global damage level, obtained as the weighted average damage of the different components (e.g. Di Pasquale and Goretti 2001; Lagomarsino et al. 2015). The mean damage of each building component is first computed, by multiplying the observed damage level, properly converted into damage states of a selected scale, by its extent. Table 3 reports the weights proposed by Lagomarsino et al. (2015) and by Di Pasquale and Goretti (2001), also adopted by Angeletti et al. (2002), for combining the damage level to a given component and the corresponding extent.

Table 3 Weights for combining damage level and extent of a given building component, for average damage-based approaches

	Level				Extent		
	D0	D1	D2–D3	D4–D5	e < 1/3	1/3 < e < 2/3	e > 2/3
Di Pasquale and Goretti (2001)	0	1	2.5	4.5	0.167	0.500	0.833
Lagomarsino et al. (2015)					0.333	0.667	1

The global average damage level of the building is then obtained by weighting the mean damage of different components (rounded to the nearest upper integer). Weights for the different building components should reflect somehow the relative cost and/or the relative importance of each element. Literature works proposed different weights, suitably differentiated for different building components and vertical structure (Table 4). For the case of masonry buildings, Lagomarsino et al. (2015), proposed to combine damage to the vertical and horizontal (both intermediate floors and roof) structural components, with weights also depending on the accuracy of the inspection (reported in the survey form). Goretti and Di Pasquale (2004) defined instead the building global damage level by considering the mean damage on the vertical bearing structure only.

An alternative approach consists in defining the building global damage level based on the maximum observed damage (e.g. Di Pasquale and Goretti 2001; Rota et al. 2008; Dolce and Goretti 2015; Del Gaudio et al. 2017). This requires converting damage descriptions in discrete damage levels of a preselected scale. Table 5 shows that the Rota et al. (2008) damage conversion rule slightly differs from the relationship by Di Pasquale and Goretti (2001). According to Lagomarsino et al. (2015), this last rule could be more appropriate than the Rota et al. (2008), where the attribution of three different damage descriptions to level DS1 may lead to a non-equally probable distribution of damage states. Taking advantage of this suggestion, this aspect was hence explored, as discussed in a following section. A different approach was proposed by Dolce and Goretti (2015), for converting the condensed damage grades of the survey form into individual levels of damage.

An additional key issue is then given by the building components to be considered for the global damage definition. Dolce and Goretti (2015) considered damage to vertical structures only, to have a similar approach for both masonry and RC buildings and to develop a simple procedure. Differently, Rota et al. (2008) considered the maximum structural damage observed among the vertical bearing structure, the horizontal structure and the roof. Although recognising the large contribution of non-structural damage to economic losses, Rota et al. (2008) used the information on non-structural damage with the only purpose of discerning cases of null structural damage from cases of incomplete survey forms. However, considering that during the Abruzzi seismic sequence, damage to RC buildings primarily concerned masonry infill panels, the information on this type of non-structural damage cannot be easily neglected. For RC buildings, Del Gaudio et al. (2017)

Table 4 Weights for the combination of the damage to the different components, to define the building mean damage level

| | Di Pasquale and Goretti (2001) | | Angeletti et al. (2002) | | Lagomarsino et al. (2015) | |
	RC	Masonry	RC	Masonry	Complete inspection	Partial/outside inspection
Vertical structure	0.300	0.350	0.70	0.70	0.60	0.80
Horizontal structure	0.225	0.275	0.05	0.10	0.20	0.0
Roof	0.225	0.275	0.05	0.15	0.20	0.20
Stairs	0.050	0.050	0.00	0.00	0.0	0.0
Masonry infills/partitions	0.200	0.050	0.20	0.05	0.0	0.0

Table 5 Damage conversion rules proposed by approaches based on the observed maximum damage (different grey shades correspond to different damage levels)

	Null	D1			D2–D3			D4–D5		
		e < 1/3	1/3 < e < 2/3	e > 2/3	e < 1/3	1/3 < e < 2/3	e > 2/3	e < 1/3	1/3 < e < 2/3	e > 2/3
Di Pasquale and Goretti (2001)	DS0	DS1	DS1	DS2	DS2	DS3	DS3	DS4	DS4	DS5
Rota et al. (2008)	DS0	DS1	DS1	DS1	DS2	DS3	DS3	DS4	DS4	DS5

defined damage levels considering the maximum damage detected on the vertical bearing structure and on masonry infills/partitions. They referred to the damage conversion rule by Rota et al. (2008) for structural damage, whereas, for masonry infills and partitions, they established a different relation between observed damage and EMS98 damage grades (i.e. DG1 corresponds to D1 in the AeDES form, DG2 corresponds to D2–D3 and DG3 to D4–D5).

3.2 Comparison of different approaches and damage conversion rules

The impact on damage distribution of different approaches and assumptions for associating the AeDES damage description with EMS98 damage levels was investigated, by applying them to the L'Aquila dataset. In mean damage-based approaches, the effect of different weights for the different building components was mainly investigated. On the other hand, considering the maximum damage definition, the impact due to consideration of structural and non-structural damage was explored. To derive empirical DPMs with different approaches, the ground motion range was subdivided into four bins of 0.075 g (Fig. 6).

Focusing on the methods based on mean global damage, DPMs were derived considering the procedure by Di Pasquale and Goretti (2001), Angeletti et al. (2002) and Lagomarsino et al. (2015). Although some literature works defined a global damage level considering damage to vertical bearing structures only (e.g. Goretti and Di Pasquale 2004; Dolce and Goretti 2015), in case of the L'Aquila seismic event, severe damage was also detected on the horizontal structures and roofs of masonry buildings (Fig. 3) and, therefore, the consideration of damage to these building components was deemed essential. Among the methods based on maximum damage, the approach by Rota et al. (2008) was initially considered.

The damage conversion rule proposed by Di Pasquale and Goretti (2001) is constrained by the damage extent indicated in the survey form, which cannot exceed 1, for each building component. As an immediate consequence, this method seems to underestimate the observed damage because, as also observed by Dolce and Goretti (2015), partial or even total collapses are not always accurately identified. The approach proposed by Lagomarsino et al. (2015) seems to be able to overcome these limitations, particularly at higher damage levels.

The definition of a global damage index suitably weighted on different building components could be more appealing for insurance purposes. Nevertheless, the different weight classification systems proposed appear to be arbitrary, although a primary differentiation is introduced between reinforced concrete and masonry buildings. The comparison of the methods based on the mean damage (black and grey shades in Fig. 6) with those considering the maximum damage (white bars in Fig. 6) shows that the latter class of
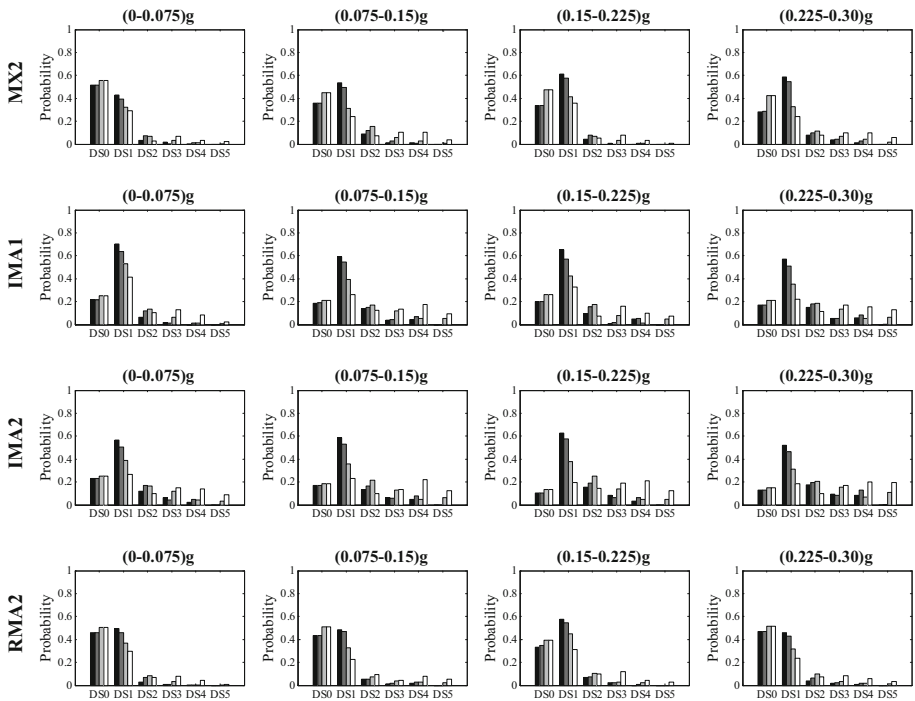
Fig. 6 Comparison of empirical DPMs of selected building typologies, for different definitions of the damage levels. Black: Di Pasquale and Goretti (2001); dark grey: Angeletti et al. (2002); light grey: Lagomarsino et al. (2015); white: Rota et al. (2008)

approaches allows to better catch all peaks of damage (Fig. 6). Although this may result in more severe damage scenarios, the maximum observed damage of the most damaged component typically determines the damage measure and therefore affects the usability outcome.

Focusing on maximum damage approaches, the comparison of the results obtained with the conversion rules by Di Pasquale and Goretti (2001) and by Rota et al. (2008) did not show significant differences. Indeed, the percent reduction (absolute value) of the probability of occurrence of DS1 obtained with Rota et al. (2008), when the Di Pasquale and Goretti (2001) conversion relationship is employed, was always lower than 10%, confirming the negligible effect of this modification.

Attention was lastly addressed to the effect of non-structural damage on masonry infills and partitions. Figure 7 compares the DPMs obtained by either neglecting (Rota et al. 2008) or considering (Del Gaudio et al. 2017) damage on masonry infills and partitions. In case of reinforced concrete buildings, the original approach by Del Gaudio et al. (2017) was applied. Differently, in case of mixed and masonry buildings (Fig. 8), this approach was modified, by defining structural damage as the maximum among the vertical bearing structure, horizontal structure and roof.

The consideration of non-structural damage seems to be important in case of reinforced concrete buildings, which generally exhibited few exemplary cases of structural collapse and countless examples of varying levels of damage to non-structural components (Braga et al. 2011; Ricci et al. 2011). Therefore, the inclusion of damage to masonry infills and
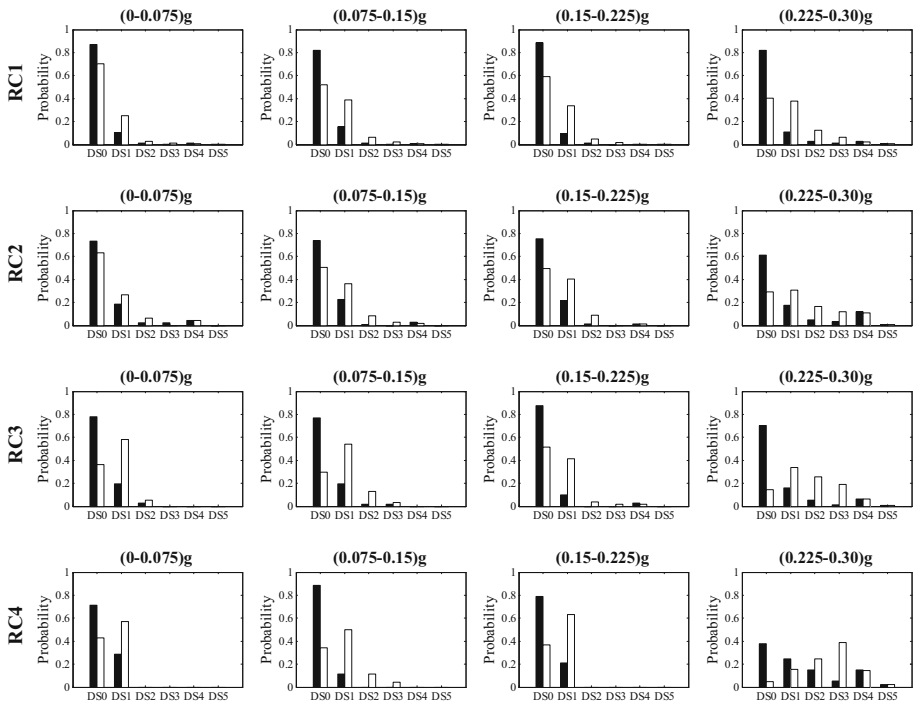
Fig. 7 Comparison of DPMs for RC building typologies, either considering (white, Del Gaudio et al. 2017) or neglecting (black, Rota et al. 2008) non-structural damage on masonry infills and partitions

partitions consistently affects the resulting damage distributions. On the other hand, this type of non-structural damage does not seem to significantly impact the damage distributions of mixed and masonry building typologies, where damage and hence usability are primarily governed by structural components (Fig. 8). The effect of this assumption will be also investigated in Sect. 4, by deriving functional loss distributions conditioned on the observed damage level.

4 Usability distributions conditional upon damage

4.1 Damage and usability assessment procedures

In the aftermath of a seismic event, damage and usability assessment is firstly addressed to the evaluation of the seismic safety conditions of damaged buildings, to allow people to return home, social and economic activities to restart and to define the number of shelters and temporary houses for homeless people (Dolce and Di Bucci 2014). In the perspective of reconstruction plans, damage and usability assessment, in combination with cost analyses, is required to determine the funds to be allocated.

In Italy, safety and damage assessment are jointly carried out, using the AeDES survey form. In many other countries, common practice is instead to carry out the safety evaluation first, by a rapid survey aiming at tagging each building by placards of different colours (e.g. JBDPA 1991; ATC 2005; Anagnostopoulos and Moretti 2008; Studer et al.
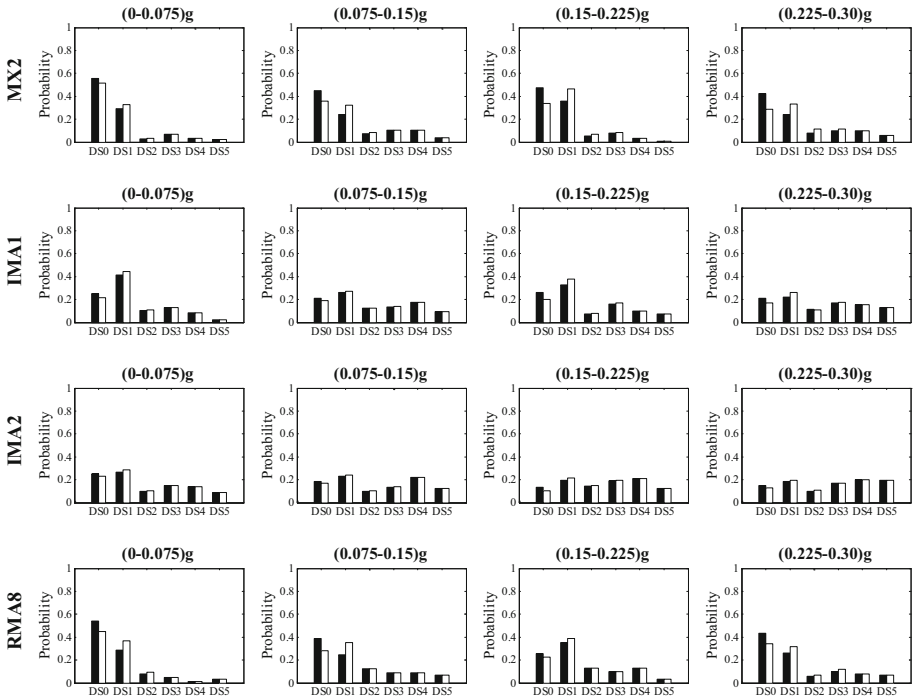
Fig. 8 Comparison of DPMs for mixed and masonry building typologies, either considering (white, Del Gaudio et al. 2017) or neglecting (black, Rota et al. 2008) non-structural damage on masonry infills and partitions

2010; NZSEE 2011). The detailed damage assessment is then launched after completing rapid surveys and it is primarily addressed to buildings with limited/restricted use and unsafe buildings.

In the framework of vulnerability assessment, usability outcomes from post-earthquake surveys could be properly processed to get a rough estimation of the functional loss of buildings, conceived as a consequence of the observed physical damage. The definition of performance, instead of damage levels, could be more appealing for both stakeholders and Civil Protection, mostly dealing with economic issues and practical activities. Along these lines, Di Pasquale and Goretti (2001) derived unusability frequency, for different vulnerability classes, by exploiting data from past Italian seismic events and considering different measures of damage, both based on mean and maximum damage definitions. The authors concluded that maximum damage definition is a better indicator than mean damage, since it is associated with the lowest frequency of unusability for DS0 and to unusability frequencies close to unit in case of DS5. Referring to the Molise 2002 seismic event, Goretti and Di Pasquale (2004) derived usability distributions conditioned on damage to the vertical bearing structure for different vulnerability classes. In this case, the authors observed the inadequacy of using damage to vertical bearing elements only, since buildings' unusability may be also driven by non-structural damage. A similar conclusion was reached by Dolce and Goretti (2015), using L'Aquila damage data to derive usability distributions conditioned on damage to vertical components and vulnerability class. Liel and Lynch (2009) examined the post-earthquake loss of functionality of a dataset of 483

RC buildings sited in the L'Aquila city, by conditioning the usability distributions on building usage, number of storeys and estimated ground motion intensity. Taking advantage of the L'Aquila usability inspections, Zucconi et al. (2017) recently proposed a model for forecasting the usability of unreinforced masonry buildings at the territorial scale, conditioned on ground motion intensity and relevant building parameters.

In the following section, the L'Aquila usability data outcomes are exploited to derive usability distributions of predefined building typologies conditioned on the observed damage levels from different measures of damage, to compare the effect of different definitions of global damage levels on the functional loss distributions of selected building typologies. Only damage measures based on maximum damage are considered for deriving usability distributions, being the usability outcome generally ruled by the maximum level of damage detected on the most damaged component. Indeed, damage measures based on average damage to the different building components were shown to overestimate damage for the lower damage levels, whereas they are not able to capture all peaks of damage and, in some cases, they miss partial or even total collapses.

4.2 Functional loss of residential buildings based on usability data

The assessment of post-earthquake usability is carried out by expert technicians in a very short time span, based on visual inspection and easily collected data. The AeDES survey form includes six possible usability outcomes (Table 6). The surveyor is also requested to indicate possible short-term countermeasures, i.e. limited, quick and easy interventions required to make the building usable.

Figure 9 shows the usability outcomes obtained from the L'Aquila dataset, subdivided by the type of vertical structure and referring to the codes reported in Table 6. Higher percentages of usable buildings (A) are observed in case of steel, mixed and reinforced concrete buildings rather than masonry constructions. The higher proportion of unusable masonry buildings (E) corroborates the higher vulnerability of this type of construction. Masonry buildings also exhibit a significant frequency of unusability due to external risk (F). As also explained by Dolce and Goretti (2015), this outcome is ascribed to the notable proportion of masonry buildings sited in historical centres, where buildings are very close one to the other and, therefore, more exposed to external risks induced by

Table 6 AeDES usability classification

| Code	Description
A—usable	Building can be used w/o measures. Small damage, negligible risk for human life
B—usable with countermeasures	Building is damaged, but can be used when short-term countermeasures are taken
C—partially usable	Only a part of the building can be safely used
D—temporarily unusable	Building requiring a more detailed investigation
E—unusable	Building cannot be used due to high structural, non-structural or geotechnical risk for human life
F—unusable for external risk	Building could be used, but it cannot due to the high risk caused by external factors
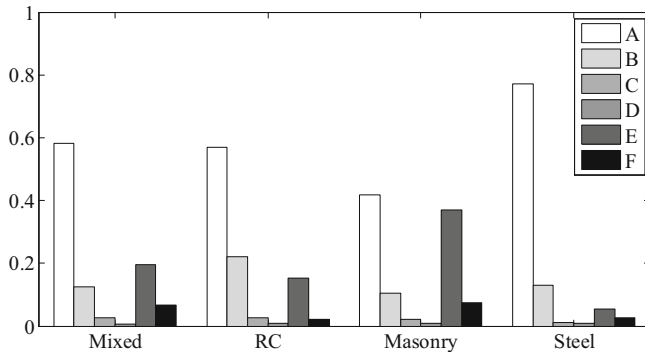
Fig. 9 Frequency of usability outcomes depending on the type of vertical structure. The meaning of the different codes (A, B, C, D, E or F) is reported in Table 6

nearby severely damaged buildings. The urbanisation settings, construction types and their distribution in the area of interest hence affect usability distributions. RC buildings show the largest fraction of outcome B, i.e. usable with countermeasures, mostly triggered by damage to masonry infills and partitions. The usability outcomes observed for mixed structures are somehow intermediate between masonry and RC buildings.

Observation of the distributions of RC and masonry buildings with outcome A, B or C and E, as a function of the number of storeys and the construction age showed that, for both structural types, the frequency of unusable buildings decreases with the age of construction, which implicitly accounts for the design code in force at the time. In more recent masonry structures (starting from 1992) this trend seems to be inverted. Only about half of the sample of 1271 new masonry buildings built after 1992 are actually "modern" buildings, meaning by that regular layout masonry buildings, with rigid diaphragms and tie-beams. By singling out only these modern buildings, the percentage of outcomes A increases from 79.4 to 89.3%, indicating that most of the recent unusable buildings are not conforming to modern standards. It should be noted that more than half of masonry buildings were built before 1920, whereas 88% of RC buildings were constructed at a relatively homogeneous rate, starting from the period 1972–1981.

Unusable buildings increase with the number of storeys, with a more continuous trend for RC structures. In this case, the number of buildings with 1, 2, 3 or 4 storeys is relatively similar, whereas for the case of masonry buildings, most of them are low-rise structures (with 95% of the buildings having less than four storeys). These findings are also in line with the observations of Di Ludovico et al. (2017), although they considered a more limited dataset of RC buildings. The comparison of the performance of modern RC and masonry structures shows that the latter have a higher percentage of usable buildings and a smaller percentage of unusable buildings, independently from the age.

L'Aquila usability data were then suitably processed to provide an estimate of the functional loss of the selected building typologies. The performance of a given building was defined as one of three possible states: usable (A), restricted/limited use (B or C) and unusable (E), similarly to the tagging systems adopted in different countries (e.g. ATC-20; NZSEE). Although constructions could be unusable when requiring a more detailed investigation (i.e. D) or due to external risk (i.e. F), buildings with code E only were taken into account. This choice is mainly related with the target of this study, i.e. comparing the fitness of different damage conversion rules for defining building global damage levels.

Two damage conversion rules were considered, i.e. the one proposed by Rota et al. (2008) and the one proposed by Del Gaudio et al. (2017), modified for the case of masonry and mixed structures as described in the following. Both are based on the maximum damage observed on different building components, with the main difference regarding the inclusion of non-structural damage to infills and partitions in the formulation by Del Gaudio et al. (2017). For the case of mixed and masonry building typologies, the Del Gaudio et al. (2017) approach, which originally defines structural damage only considering vertical structures, was modified, by defining structural damage as the maximum among vertical structure, horizontal structure and roof, since damage to these structural elements appeared to be non-negligible. On the other hand, for RC buildings, the formulation by Del Gaudio et al. (2017) was adopted in its original formulation. Figure 10 shows the usability distribution conditioned on the global damage levels, obtained with the two damage conversion rules, for the different RC building typologies. In the plots, white represents usable buildings (A), grey indicates buildings with restricted/limited use (B and C) and black is for unusable buildings (E). Similarly, Fig. 11 shows usability distributions for some masonry building typologies.

In general, the fraction of usable buildings significantly decreases starting from damage level DS2, independently of the building typology. Most of the buildings are unusable at higher damage levels, particularly starting from damage level DS3. The presence of unusable buildings, even when no structural damage is observed and non-structural damage is accounted for (i.e. in the formulation by Del Gaudio et al. 2017), is explained by geotechnical risks and pre-existing damage. The comparison of the adopted damage conversion rules shows that structural damage mainly governs the functional loss of masonry buildings. It is indeed observed that the consideration of damage to internal partitions does not significantly impact the resulting functional loss distributions, which seem to be only slightly affected at the lowest damage level. Differently, the consideration of damage to masonry infills and partitions has a significant effect in case of reinforced concrete structures. Indeed, when structural damage only is considered for defining global damage levels (i.e. in the approach by Rota et al. 2008), non-negligible unusability frequencies are observed for DS0. This issue is improved by adopting the Del Gaudio et al. (2017) damage conversion, which also considers non-structural damage.
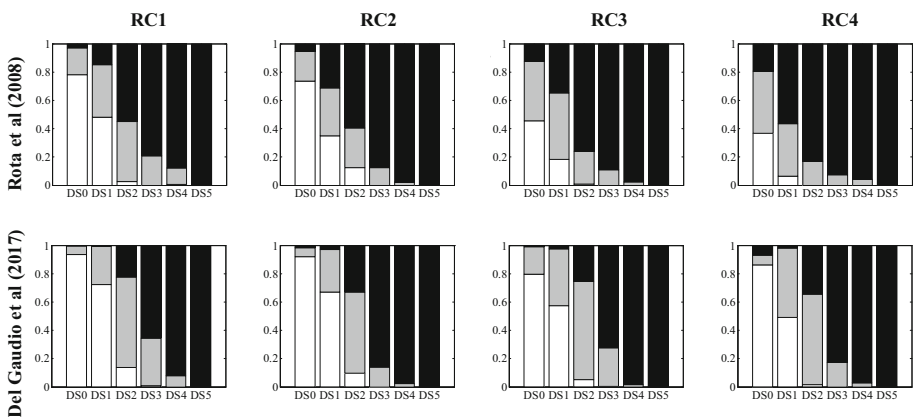

Fig. 10 Distributions of usability outcomes for different RC building typologies, using the Rota et al. (2008) damage conversion rule (top) and the Del Gaudio et al. (2017) damage conversion rule (bottom). White: usable buildings (usability outcome A); grey: buildings with restricted/limited use (outcomes B and C); black: unusable buildings (outcome E)
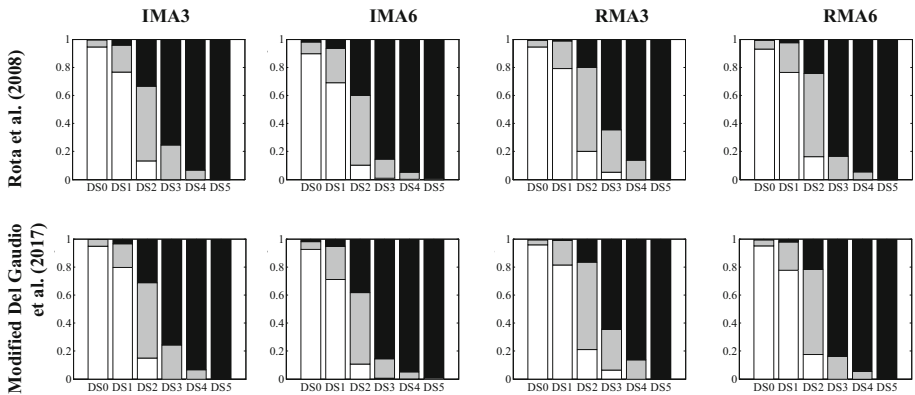
Fig. 11 Distributions of usability outcomes for different masonry building typologies, using the Rota et al. (2008) damage conversion rule (top) and the modified Del Gaudio et al. (2017) damage conversion rule (bottom). White: usable buildings (usability outcome A); grey: buildings with restricted/limited use (outcomes B and C); black: unusable buildings (outcome E)

5 Considerations on the distribution of damage in the different damage states

Damage probability matrices of several building typologies exhibited a bimodal trend (Fig. 8), that appeared to be insensitive to the adopted definition of damage levels (based on maximum damage). The data present disproportionate probabilities of occurrence of the lowest damage states, independently of the ground motion intensity level. This could be related to the nature of empirical data, in which similar effects could be due to misclassification errors, to the inexperience of the surveyors (with difficulties when assessing lighter damage states), or to bias in the data collection (e.g. Rossetto et al. 2013). It could be also explained by the possible presence of some pre-existing damage, which is even more difficult to be assessed at the lower damage levels. These existing structural and non-structural defects can be aggravated by the seismic event and, if unaccounted for, may bias damage and loss prediction models (Maffei et al. 2006; Zucconi et al. 2017). Past works recognised the issue represented by pre-existing damage (e.g. Di Pasquale and Orsini 1997; Rota et al. 2008) and tried to address it by exploiting the information provided by the AeDES form, in which the presence of pre-existing damage and its extent can be indicated referring to the whole building (e.g. Goretti and Di Pasquale 2004; Dolce and Goretti 2015). Nevertheless, in many practical cases, it is difficult for a surveyor to distinguish the portion of pre-event damage from the damage due to the seismic event and therefore this information in the survey form is not very reliable.

Starting from these considerations, this paper proposes two hybrid approaches, to interpret and account for the bimodal trend of damage repartition in the different states. Examples of application are then outlined to show the feasibility of both methods, pointing out pros and weaknesses of each procedure. Based on the observations reported in the previous sections, the damage measure proposed by Del Gaudio et al. (2017) was adopted for RC buildings, since it accounts for non-structural damage, whose consideration is particularly relevant for this type of structures. On the other hand, the damage measure by Rota et al. (2008) was used for masonry and mixed buildings, as it is based on maximum damage to vertical structure, horizontal structure and roof (rather than only vertical

structure). For this kind of structures, indeed, consideration of damage to masonry infills and partitions does not significantly affect the damage distribution, whereas damages to horizontal structure and roof were often observed.

5.1 Proposals to account for the bimodal repartition of damage into damage states

Empirical damage data can be represented in the form of histograms, expressing the probability of occurrence of the different damage states, for a preselected ground motion intensity level. Probability distributions can be then used to fit these histograms, providing a continuous representation of the seismic vulnerability and making empirical data easily usable for other vulnerability or risk applications. Literature works showed that the binomial model can fairly well approximate damage distributions resulting from post-earthquake data (e.g. Braga et al. 1982; Sabetta et al. 1998; Roca et al. 2006). The simplicity of the binomial distribution is that the entire distribution of buildings in the different damage levels can be expressed by a single parameter, μ_D, representing the value of mean damage of the discrete damage distribution. On the other hand, it does not allow to define the scatter of the damage levels around the mean value.

According to the binomial distribution, the number of buildings N_k, experiencing damage level DS_k, can be expressed as:

$$N_k = N_{tot} \frac{n!}{k!(n-k)!} \left(\frac{\mu_D}{n}\right)^k \left(1 - \frac{\mu_D}{n}\right)^{n-k} \tag{1}$$

where N_{tot} is the total number of buildings in the considered ground motion interval, n is the number of damage levels and k varies from 0 to n. The mean damage value of the discrete damage distribution, μ_D, can be derived by combining the probabilities of having the different damage states:

$$\mu_D = \sum_{k=0}^{n} \frac{N_k}{N_{tot}} k \tag{2}$$

Figure 12 compares the observational damage distributions (black bars) derived for building typology IMA6 (selected as an example), using the damage scale proposed by Rota et al. (2008), with the prediction obtained by the binomial distribution (grey bars). It can be observed that, in this case (but this observation can be extended to several other building typologies), imposing the binomial fitting of damage probability matrices on all data does not seem to provide satisfactory approximations, as it is not able to reproduce the bimodal repartition of damage into the different levels, with a trend for damage states DS0–DS1 and a different trend for higher damage levels.

Therefore, it was decided to look for the binomial model better approximating empirical damage distributions, for damage levels from DS2 to DS5 only. Since buildings with no damage (DS0) and with negligible to slight damage (DS1) are hence not initially included in the binomial approximation, the total number of buildings binomially distributed does not correspond to the total number of buildings in the ground motion interval of interest, but it is unknown. Therefore, the optimisation problem has two unknowns, i.e. the number of buildings following the binomial model (N_{tot}) and the mean damage of the binomial distribution (μ_D). Once these two parameters are optimised by the combined use of Eqs. (1) and (2) and by minimising the sum of the squared errors between predictions and
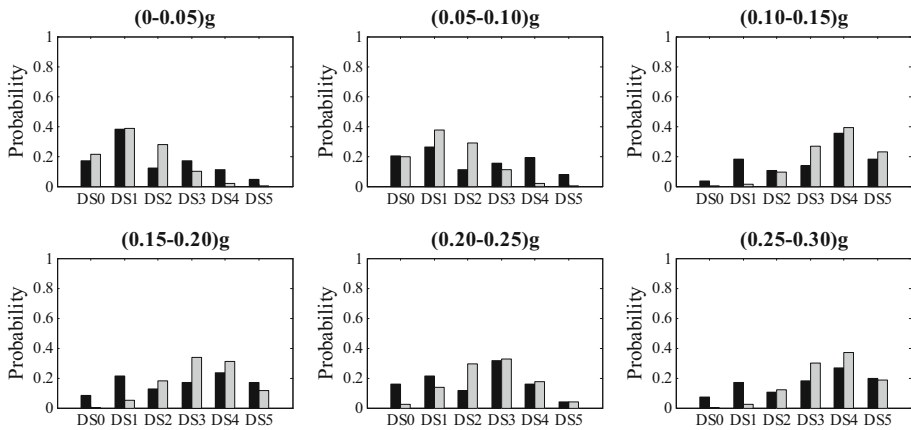
Fig. 12 Comparison of empirical DPMs (black) and binomial prediction (grey) for building typology IMA6 (4229 buildings)

observations, the number of buildings suffering DS0 and DS1 in accordance with the binomial prediction is also derived. The fitting procedure is carried out by satisfying the constraint for which the predicted and observed number of buildings experiencing damage states from DS2 to DS5 should be equal. This condition allows to identify the fraction of buildings with observed damages DS0 and DS1 deviating from the imposed binomial model.

The fraction of non-binomially distributed buildings is then treated separately from the rest of buildings, which instead follow the binomial model. The percentage of non-binomially distributed buildings could be fitted as a function of the preselected ground motion intensity measure, by considering appropriate analytical functions, hence providing continuous estimates for all ground motion intensity values. On the other hand, the repartition of binomially distributed buildings in the different damage levels could be represented by a single parameter (μ_D), as a function of the selected intensity measure, similarly to other studies (e.g. Lagomarsino and Giovinazzi 2006; Rota and Rosti 2017; Rosti and Rota 2017). This would provide a continuous and concise representation of the vulnerability as a function of the ground motion IM.

The combination of the information on buildings deviating from the binomial model with those binomially-distributed allows to derive damage distributions for each ground motion intensity. A scheme of the different phases of the proposed methodology is depicted in Fig. 13. As illustrated, a final step could then envisage the further processing of the obtained damage distributions to derive fragility curves. Despite its simplicity, the approach previously outlined allows to provide reliable and quite accurate predictions for higher damage states (i.e. from DS2 to DS5). By contrast, although a fraction of buildings experiencing damage states DS0 and DS1 and deviating from the binomial model can be identified, the procedure does not allow identifying the actual repartition of buildings between undamaged (DS0) and slightly damaged (DS1).

Several interpretations could justify the fraction of buildings which are not binomially distributed. A possible explanation could be given by the presence of pre-existing damage, which mainly affects damage state DS1, although even the higher damage levels might be interested, as any level of pre-event damage can be aggravated by the seismic event. Also,
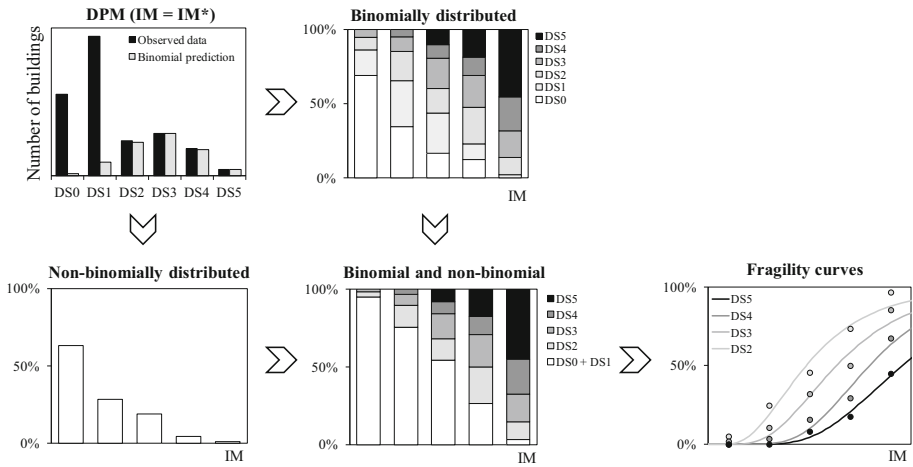
Fig. 13 Sketch of the first proposed procedure to account for the bimodal trend of damage levels distribution

the impact of pre-existing damage is likely to be more significant at lower ground motion intensity levels.

At higher ground motion intensities, the presence of buildings deviating from the binomial model could be explained for example by the fact that damage probability matrices are derived by grouping together buildings with similar characteristics. Nevertheless, the damage repartition can be heterogeneous even within the same building typology, due to the presence of buildings with structural or architectural features which are not taken into account by the adopted typological classification or by the survey form. In case of masonry buildings, for example, the adopted taxonomy contemplates some structural characteristics (i.e. type of vertical and horizontal structures, number of storeys and presence of tie-rods and/or tie-beams), whereas other vulnerability parameters, such as material quality (in particular mortar properties), different construction details, architectural configurations, walls and openings distributions and soil conditions are not accounted for. All these characteristics, escaping the considered typological classification system, contribute to the sample heterogeneity in terms of vulnerability. Other factors impacting damage repartition may also concern the relatively coarse definition of the seismic input (at the municipal level) and the uncertainties related to the adoption, as an intensity measure, of PGA on rock obtained from a GMPE.

On the other hand, some non-null probabilities of occurrence of damage level DS5, even at low ground motion intensity levels, were surprisingly observed. These probabilities could be explained by the possible presence of buildings which were intrinsically extremely vulnerable (or, in some cases, even prone to collapse before the occurrence of the earthquake) due to inadequate layout, poor quality and lack of constant maintenance. This is in accordance with Galli et al. (2009), based on observations of groups of stone masonry buildings completely abandoned, and even partially ruined, before the same seismic event, standing in the historical centres of several Abruzzi localities. Similarly, the poor seismic performance of some masonry constructions, due to overall layout, construction details and poor maintenance, was observed during post-earthquake surveys after the 2012 Emilia seismic events (e.g. Sorrentino et al. 2014).

To overcome some limitations of the first procedure, a second approach was developed, to capture the bimodal repartition of damage in the different levels of Rota et al. (2008), providing information on the distribution of all damage states. The procedure takes advantage again of the binomial model but, in this case, two binomial distributions are jointly considered to approximate empirical DPMs. The first binomial distribution is aimed at capturing the trend of buildings with damage states DS0 and DS1 and it is fully described by its mean damage grade, $\mu_{D,1}$, and the number of buildings, $N_{tot,1}$. Differently, the second binomial distribution is defined to better catch the damage repartition at higher states (i.e. from DS2 to DS5) and is fully defined by its mean damage grade, $\mu_{D,2}$, and the number of buildings following this model, $N_{tot,2}$. The number of buildings of the two binomial distributions, $N_{tot,1}$ and $N_{tot,2}$, are dependent, since their sum must to be equal to the total number of constructions in the considered ground motion intensity range, N_{tot}. For each level of damage, the predicted probability of occurrence is then given by the sum of the frequencies obtained from the two binomial models. The two binomial distributions are jointly fitted on the empirical data, by minimising the sum of the squared errors between predictions (of the whole model) and observations. Optimal independent parameters (e.g. $N_{tot,1}^{opt}$, $\mu_{D,1}^{opt}$ and $\mu_{D,2}^{opt}$) are hence derived. The main phases of the outlined approach are sketched in Fig. 14, with reference to a general ground motion intensity interval, *IM**.

The percentage of buildings following the first and second binomial models can be fitted by continuous analytical functions, as a function of the preselected ground motion intensity measure. For each value of ground motion intensity, the combination of the information on buildings binomially distributed according to the two models, with the corresponding mean damage values, allows predicting the overall damage distribution. This second procedure has the unquestionable advantage of providing estimates for all levels of damage, with a fairly good approximation of all the observed probabilities.

5.2 Application to the case study of a masonry building typology

This section presents examples of application of the outlined methodologies to a masonry building typology case study, consisting of irregular layout or poor-quality masonry with flexible diaphragms and more than two storeys, without tie-rods and tie-beams (IMA6, Table 1). The damage scale adopted in this section is the one proposed by Rota et al. (2008).

Figure 15 shows the binomial prediction of the observed number of buildings (grey bars) undergoing different damage states, obtained with the first procedure, i.e. imposing the binomial distribution to approximate empirical data on damage levels from DS2 to DS5. Given the significant differences in terms of number of buildings in the different PGA bins, the scale of the vertical axis is not kept constant.
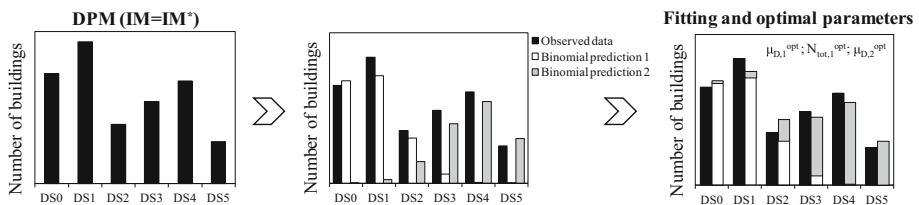

Fig. 14 Sketch of the second procedure to account for the bimodal trend of damage levels distribution
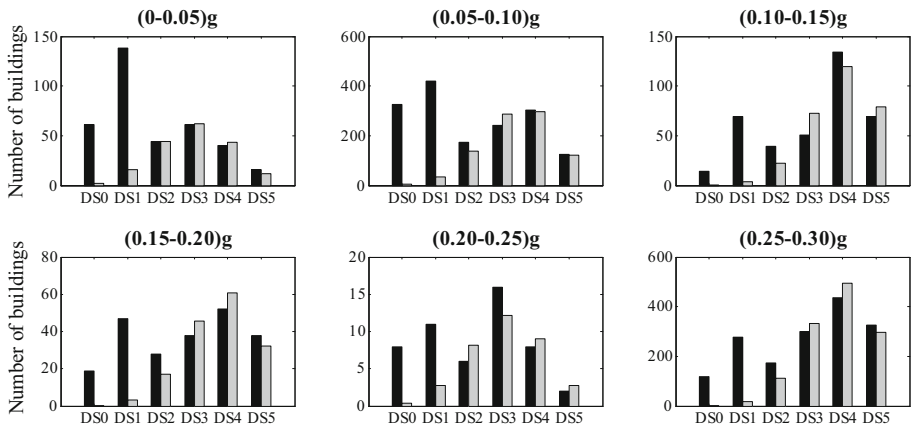
Fig. 15 Comparison of the observed (black) and predicted (grey) number of buildings, by imposing the binomial model on damage levels from DS2 to DS5 (IMA6)

For each PGA interval, fractions of binomially and non-binomially distributed buildings were identified. Figure 16 (left) shows the proportion of non-binomially distributed buildings, as a function of PGA. Results were fitted by a logarithmic regression line, continuously describing the trend of data as a function of PGA:

$$y = b_1 \ln(PGA) + b_2 \tag{3}$$

where b_1 and b_2 are the regression coefficients, equal to -0.11 and 0.09, respectively, for this specific case.

Figure 16 (centre) shows the repartition of binomially-distributed buildings into the different damage levels. The mean damage of the binomial distribution, μ_D, was selected as a global damage indicator (white squared markers) and, for each PGA bin, it was computed as the weighted average of the expected probabilities of the different damage states (Eq. 2). A continuous PGA-μ_D relationship (white continuous line) was derived by imposing a logarithmic regression model on the data points. As expected, the mean damage tends to (slightly) increase with the ground motion intensity level. The analytical relationship between μ_D and PGA can be hence expressed as:

$$\mu_D = a_1 \ln(PGA) + a_2 \tag{4}$$

where the regression coefficients, a_1 and a_2, turned out to be equal to 0.24 and 3.93, respectively.

Taking advantage of the continuous regression lines, hybrid damage distributions were derived for each value of PGA, starting from 0.025 g (Fig. 16, right). In the figure, damage repartition is accurately defined for damage states from DS2 to DS5. Differently, no distinction is provided in case of buildings suffering damage states DS0 and DS1, as the identification of non-binomial buildings does not allow identifying the actual damage repartition at these lower damage levels. The obtained results, providing a continuous representation of the vulnerability as a function of the ground motion shaking, could be subsequently processed to derive fragility curves (that can be obtained as one minus the probabilities represented in Fig. 16, right).

To forecast data distribution in all damage states, the second approach was then applied. Figure 17 shows the comparison of empirical DPMs (black bars) and predictions resulting
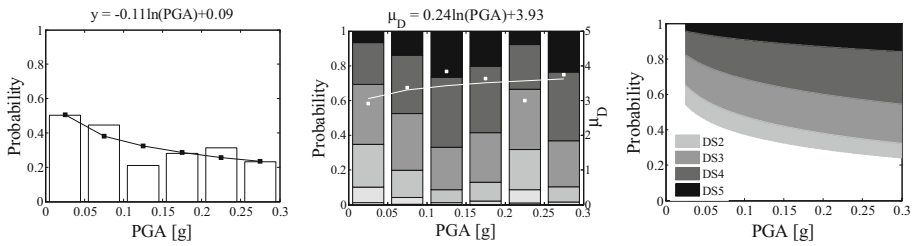
Fig. 16 Non-binomially distributed buildings as a function of PGA (left), repartition of binomially-distributed buildings into different damage levels (centre) and continuous hybrid damage distributions (right), for building typology IMA6
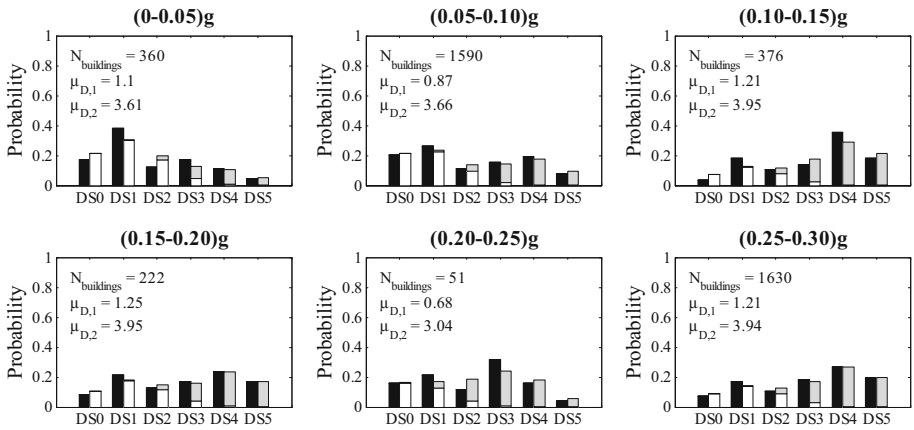

Fig. 17 Comparison of empirical DPMs (black) with predictions obtained for building typology IMA6 with the second procedure, differentiated based on the contribution provided by each considered binomial distribution. White bars correspond to the first binomial distribution, well approximating the lower damage levels; grey bars indicate the second binomial distribution, better describing higher damage states

from the joint use of the two binomial distributions. In particular, white bars correspond to the binomial distribution well approximating the trend of lower damage levels, whereas grey bars indicate the binomial distribution better describing higher damage states. In general, it is observed that the sum of the two distributions provides a quite good approximation of observational data at all damage states, which is a significant advantage with respect to the previous approach.

For each PGA interval, the optimisation procedure provides the fraction of buildings following each of the two binomial distributions. This trend was fitted by a logarithmic regression line (Fig. 18, left). The figure shows that the percentage of buildings following the first binomial distribution (white bars) tends to reduce with the increase of the ground motion intensity. The central part of Fig. 18 shows, instead, the mean damage values associated with each binomial distribution, for each predefined PGA interval. The mean damage values seem to oscillate around a constant value and it is hence possible to identify constant regression lines (dashed lines). By knowing the percentage of buildings following each binomial distribution and the value of the constant regression lines, hybrid damage distributions can be then obtained for all ground motion values in the range of interest
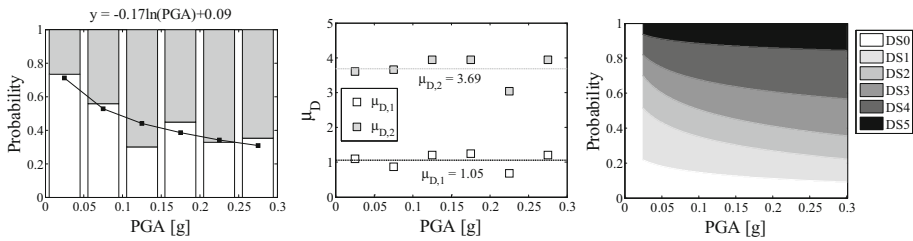
Fig. 18 Logarithmic fitting of the fraction of buildings following the first (white bars) binomial distribution (left), for building typology IMA6; mean damage values defining the two binomial distributions (centre) and continuous hybrid damage distributions (right)
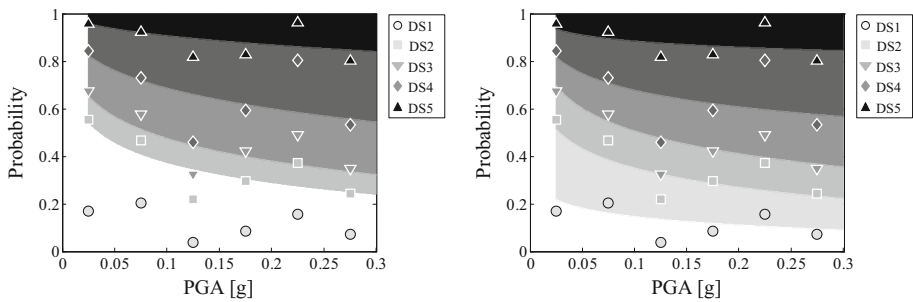

Fig. 19 Comparison of empirical damage data with continuous hybrid damage distributions derived for building typology IMA6 by applying the first (left) and second (right) procedure

(Fig. 18, right). The trend of the resulting hybrid damage distributions as a function of PGA is produced by the decreasing number of buildings following the first binomial model for increasing PGA values.

Figure 19 plots empirical damage data against the continuous hybrid damage distributions, resulting from both approaches. The major difference between the two figures concerns the prediction of the probability of occurrence of DS0 and DS1, which is only feasible with the second procedure. The trend of the other damage states as a function of PGA is similar, although some differences can be visually detected. For instance, the probability of occurrence of DS3 is slightly higher with the first approach (Fig. 19, left). Differently, the expected probability of occurrence of damage state DS2 is larger with the second procedure (Fig. 19, right). However, this is just a qualitative comparison, based on the simple observation of the obtained results. Looking at empirical data points, it can be curiously noted that, in the 0.2–0.25 g range, the observed damage is less severe than expected. However, this outcome may lack reliability due to the relatively small number of data available in this interval of ground motion intensity (Fig. 2).

5.3 Accuracy of different approaches to approximate empirical damage distributions

The previous section highlighted the feasibility of the outlined procedures to approximate empirical damage distributions, with reference to a case study. The suitability of each method was qualitatively assessed, by comparing advantages and weaknesses. The preliminary comparison pointed out that the methodologies work and produce quite reliable
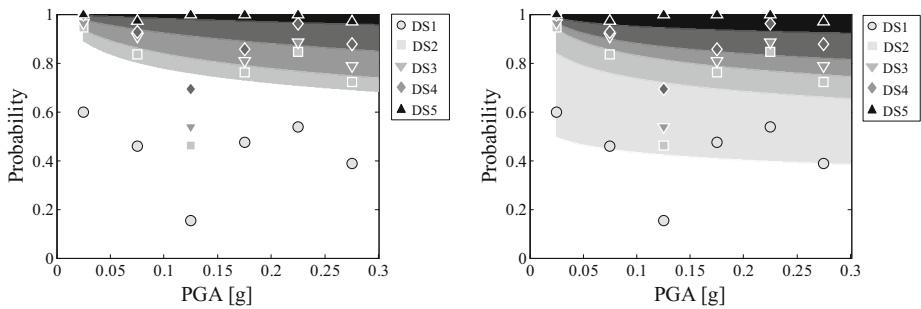
Fig. 20 Comparison of empirical damage data (Rota et al. 2008 damage scale) with continuous hybrid damage distributions derived by applying the first (left) and second (right) procedure—building typology RMA5 (Table 1)

predictions, provided that observational damage data are available and sufficient. Figure 20 shows an example where the two hybrid procedures work, but the distribution of scarce empirical data in the different PGA bins affects the credibility of the resulting hybrid distributions. This aspect is particularly evident in case of damage level DS5, where the second hybrid procedure seems to overpredict the observations (Fig. 20, right).

To uniformly and quantitatively assess the accuracy of each method (i.e. the classical binomial model and the two proposed hybrid approaches) and to identify the one with the best global performance, a synthetic error parameter was defined. For each damage level, the mean absolute percentage error between empirical and expected probability of occurrence of each damage level was computed, for each building typology, by averaging (over the PGA range) the absolute percentage errors evaluated at different PGA thresholds. The synthetic error parameter was then defined as the square root of the ratio of the sum of squares of the mean absolute percentage errors, obtained for different damage states, and the number of the considered damage levels. In case of the first approach, damage levels DS0 and DS1 were considered together, given that the approach does not allow to get specific estimates for these damage states.

In this comparison, steel constructions were excluded due to scarce data, non-uniformly spread in the different ground motion intensity bins. In case of RC building typologies, empirical DPMs were derived by applying the damage conversion rule by Del Gaudio et al. (2017), deemed to be more appropriate for this type of constructions (Sect. 4.2).

Figure 21 shows the mean absolute percentage error of the probability of occurrence of the different damage states, according to the classical binomial model and the two proposed hybrid approaches. To make the three approaches comparable, a μ_D-PGA continuous relationship was derived from the prediction obtained with the classical binomial model, by adopting a logarithmic regression model (similar to that in Eq. 4).

In the figures, white markers refer to the classical binomial fitting on all damage data, grey markers correspond to the first hybrid approach (i.e. binomial model imposed on damage levels from DS2 to DS5), whereas black markers refer to the second procedure, where two binomial distributions are jointly imposed on empirical damage data. The mean absolute percentage errors of damage levels DS0 and DS1 could not be computed for the first hybrid approach (grey markers), for the limitations intrinsic in the method. Also, it should be noted that, in some cases, markers are missing for some damage levels and/or for some building typologies. This indicates that, in this specific case, the corresponding
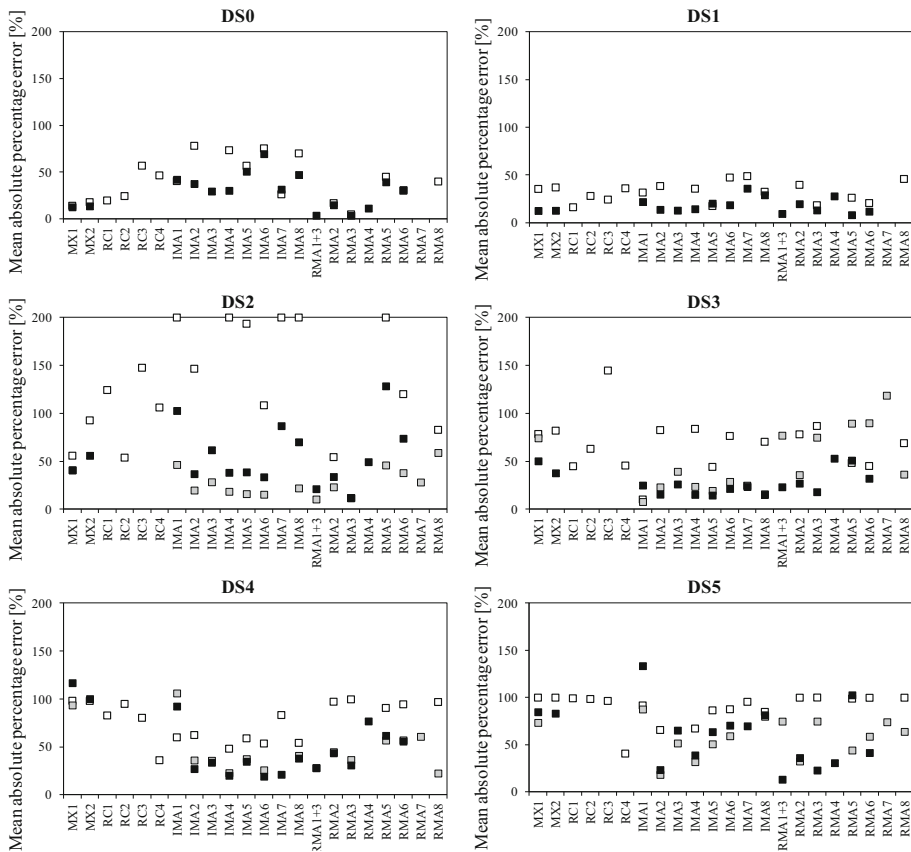
Fig. 21 Comparison of the mean absolute percentage error between the observed and predicted probabilities of occurrence of all damage states. Predictions are derived from the classical binomial fitting on all damage data (white), from the first (grey) and second (black) hybrid approaches

procedure could not be successfully implemented, for the reasons discussed in the following.

In case of DS2, some considerably high percentage errors were found with the classical binomial approach; in this case, for graphical reasons, percentage errors in the plots were limited to a threshold of 200%. These high values, mainly regarding masonry typologies, are related to the non-binomial trend observed in the data, which is more evident for this damage level (Fig. 12).

For RC building typologies, hybrid procedures cannot be successfully implemented due to the lack of data with higher damage levels (implying the impossibility of imposing a binomial distribution on higher damage levels, in accordance with the first procedure) or to a (physically inconsistent) non-increasing mean damage trend as a function of PGA. The former issue is also explained by the significant number of data falling in the 0.25–0.30 g bin, whereas the latter could be due to the poor correlation between the peak ground acceleration and the observed seismic damage, and it could be improved by introducing a different intensity measure, at least for high-rise RC buildings, for which a spectral parameter in the constant velocity portion of the spectrum could be more suitable. In mixed

building typologies, hybrid approaches generally show more accurate predictions than the classical binomial model.

For irregular layout or poor-quality masonry building typologies (IMA), the implementation of the proposed hybrid approaches generally reduces the discrepancy between observations and predictions, especially starting from damage level DS1, whereas the binomial prediction and those obtained from the second hybrid approach are comparable at damage level DS0. At DS2, the first hybrid approach is more accurate than the second one, but at some of the higher damage states, the errors of the two hybrid approaches are comparable.

In case of regular layout and good-quality masonry buildings (RMA), similar errors are obtained at damage states DS0 and DS1 from the traditional binomial model and the second hybrid procedure. At DS2, the first hybrid procedure confirms its larger accuracy with respect to the other approaches, whereas at higher damage levels, both the hybrid approaches generally allow to get smaller errors than the binomial model. In some building typologies (i.e. RMA7 and RMA8), the successful implementation of the second approach was impeded by the presence of some damage distributions which could be easily represented by two binomial distributions and some where the two binomial distributions collapsed into a single one. In other typologies (e.g. RMA1), the application of the hybrid procedures was not successful, due to the lack of data with higher damage levels, impeding the binomial fitting on DS2–DS5, or to a non-increasing mean damage trend as a function of PGA.

Table 7 reports the values of the considered synthetic error parameter, calculated for each typology with the three considered approaches, highlighting by bold characters the approach providing the best fit to the empirical data (i.e. the lowest error parameter). The cases in which the error parameter is not reported are those for which the corresponding approach does not provide satisfactory results, for one of the reasons discussed above. It can be noted that building typology RMA1 was replaced in Table 7 by typology RMA1 + 3, which includes buildings falling in both typologies RMA1 and RMA3, i.e. neglecting the information on diaphragms' flexibility. This was required because the data belonging to RMA1 were not covering all damage levels and PGA intervals in a sufficiently uniform way.

For each typology, Table 7 also reports the parameters of the equations required to apply the selected best fitting approach. In particular, for the classical binomial approach and for the first hybrid approach, the parameters a_1 and a_2 are used to derive μ_D as a function of PGA (Eq. 4). In addition, for the first hybrid approach, b_1 and b_2 are the parameters to derive continuous relationships between PGA and the fraction of non-binomially distributed buildings, y (Eq. 3). Referring to the second procedure, a_1 and a_2 correspond to $\mu_{D,1}$ and $\mu_{D,2}$, i.e. the mean damage values of the constant regression lines corresponding to the two binomial distributions, whereas b_1 and b_2 are the parameters describing the trend of buildings following the first binomial distribution as a function of PGA. The provided parameters could be used to derive hybrid damage distributions for each value of ground motion in the PGA range 0.025–0.30 g, allowing to predict seismic damage due to future earthquakes in areas with similar seismotectonic characteristics and built environment.

Finally, Fig. 22 reports, for each building typology, the DPMs obtained with the best fitting approach identified by bold characters in Table 7 and the corresponding empirical points for the different damage levels. The colour of the frame of each subfigure indicates the best fitting approach: no frame for the classical binomial distribution; grey frame for approach 1 and black frame for approach 2.

Table 7 Comparison of values of the considered synthetic error parameter obtained from the three approaches and parameters of the "best" selected model (identified by bold numbers), for each building typology

| | Error parameter | | | Parameters of the selected model* | | | |
	Binomial	Approach 1	Approach 2	a_1	a_2	b_1	b_2
MX1	0.71	0.65	**0.65**	0.43	3.51	− 0.07	0.70
MX2	0.78	–	**0.60**	0.45	3.49	− 0.06	0.67
RC1	**0.76**	–	–	0.08	0.74	–	–
RC2	**0.67**	–	–	0.14	0.96	–	–
RC3	**1.02**	–	–	0.04	1.02	–	–
RC4	**0.57**	–	–	0.75	3.08	–	–
IMA1	1.42	**0.66**	0.81	0.29	3.74	− 0.09	0.34
IMA2	0.86	**0.24**	0.27	0.19	3.89	− 0.09	0.18
IMA3	–	**0.36**	0.43	0.14	3.46	− 0.07	0.48
IMA4	1.08	**0.23**	0.28	0.17	3.89	− 0.04	0.30
IMA5	0.95	**0.33**	0.41	0.26	3.78	− 0.10	0.23
IMA6	0.78	**0.33**	0.45	0.24	3.93	− 0.11	0.09
IMA7	1.41	–	**0.51**	0.83	3.61	− 0.03	0.53
IMA8	1.20	0.45	**0.52**	0.99	3.79	− 0.03	0.41
RMA1 + 3	–	0.50	**0.18**	0.33	3.58	− 0.02	0.90
RMA2	0.71	0.31	**0.31**	0.53	3.43	− 0.06	0.66
RMA3	0.68	0.50	**0.19**	0.29	3.48	− 0.02	0.91
RMA4	–	–	**0.47**	0.37	3.39	− 0.05	0.74
RMA5	1.58	**0.56**	0.76	0.36	3.75	− 0.08	0.57
RMA6	0.78	0.57	**0.45**	0.78	4.20	− 0.05	0.69
RMA7	–	**0.69**	–	0.43	2.97	0	0.88
RMA8	0.76	**0.44**	–	0.48	3.74	− 0.06	0.55

*The reported parameters must be used consistently with the selected model

Classical binomial model: $\mu_D = a_1 \ln(PGA) + a_2$

Approach 1: $\mu_D = a_1 \ln(PGA) + a_2$; $y = b_1 \ln(PGA) + b_2$

Approach 2: $\mu_{D,1} = a_1$; $\mu_{D,2} = a_2$; $z = b_1 \ln(PGA) + b_2$

6 Conclusions

This work presents an in-depth study on the effects of different damage classifications on the empirical seismic vulnerability of building typologies, representative of the Italian building stock. The study is based on a wide and homogeneous database of post-earthquake damage data, collected in a specific region of the Apennines, after the L'Aquila seismic event of 2009.

Manifold aspects and issues related to damage descriptions and definitions were thoroughly explored. As a starting point, two types of approaches, commonly adopted in the literature to assign damage levels to each inspected building, were reviewed. The first class of methods defines global damage levels as the weighted average of the mean damage observed on different building components. By contrast, the second approach defines
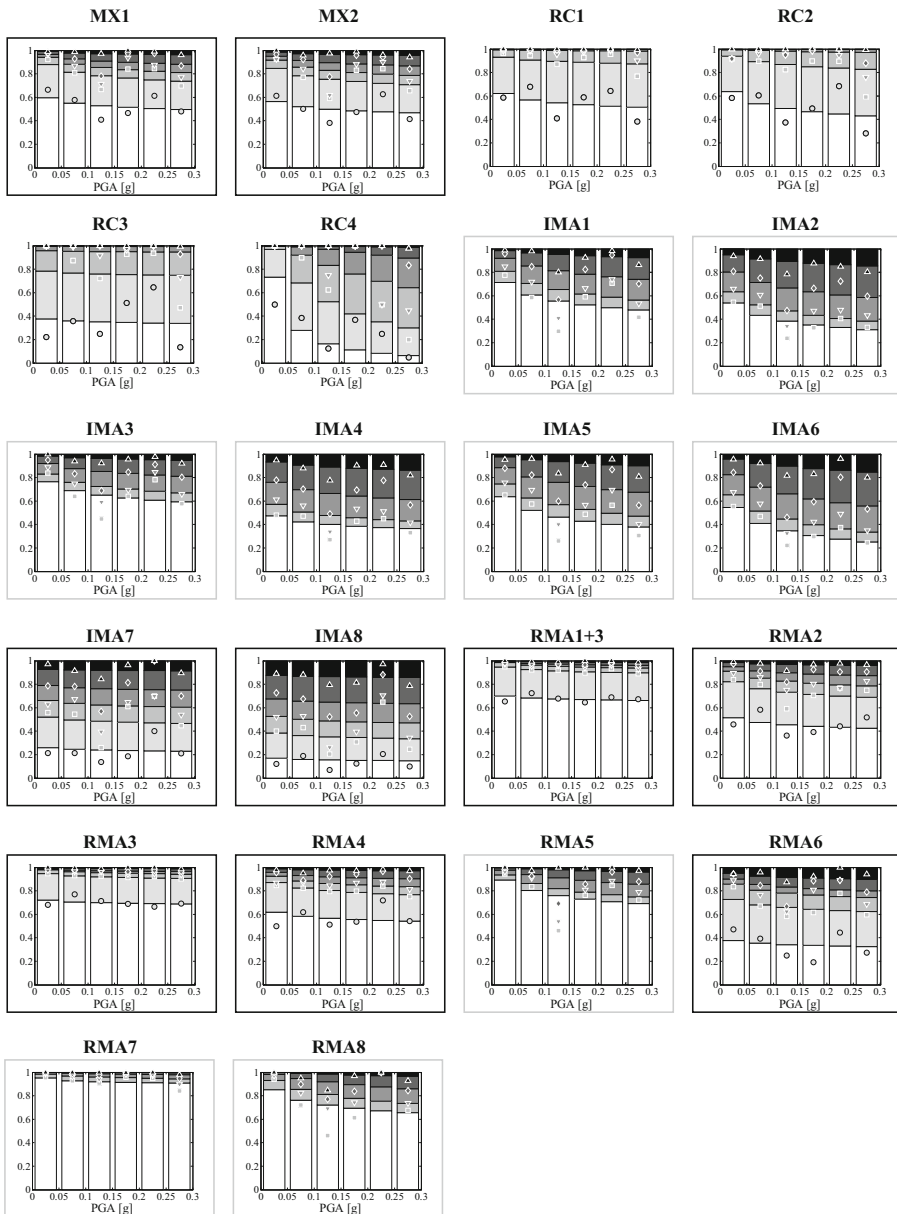
Fig. 22 Damage probability matrices obtained, for each building typology, with the selected model (Table 7) and comparison with observed damage data. No frame: classical binomial distribution; grey frame: approach 1 and black frame: approach 2. In case of approach 1, markers corresponding to observed DS1 are not reported, as the method is unable to distinguish DS0 and DS1

damage levels based on the maximum damage detected on some preselected building components. Empirical damage distributions pointed out the tendency of the mean damage-based approaches to underestimate the actual observed damage, since they do not

allow to accurately account for partial and total collapses. Moreover, the definition of weights for the different building components bears subjectivity and uncertainty. On the other hand, approaches based on maximum observed damage allow capturing all peaks of damage and seem more appropriate, also because the maximum observed damage of the most damaged building component typically drives the usability rating.

Considering the significant role of non-structural damage in recent earthquakes worldwide, the inclusion of masonry infills and partitions in the definition of damage levels was explored, both in terms of resulting DPMs and functional loss conditioned on damage states. Results demonstrated the appropriateness of including damage to masonry infills and partitions in case of RC buildings, for which the observational evidence showed that damage to these building components causes injuries, direct economic losses and often impedes building's functionality (Braga et al. 2011; Ricci et al. 2011). By contrast, damage detected on masonry partitions did not seem to govern the definition of damage levels in case of unreinforced masonry buildings and mixed constructions, where building damage was primarily dominated by structural damage on vertical bearing walls and floor and roof diaphragms. In these cases, the consideration of damage to internal partitions slightly affected the lowest damage level only.

The impact of different definitions of damage was also studied with reference to distributions of the usability outcomes of predefined building typologies, conditioned on the observed damage levels. This study showed that recently constructed unreinforced masonry buildings are less vulnerable than older constructions, confirming the observations of other post-earthquake field surveys (e.g. Saatcioglu and Bruneau 1993; Penna et al. 2014).

Damage probability matrices of several building typologies, derived by considering the maximum damage-based approach, exhibited a bimodal repartition of damage in the different levels. In particular, damage distributions presented a high probability of occurrence of damage level DS1, with respect to the other states. As discussed by Rossetto et al. (2013), this outcome could be ascribed for example to misclassification errors, or inexperienced surveyors with difficulties when assessing lower damage levels. A further explanation could be the possible presence of some pre-existing damage, particularly in case of masonry buildings, often lacking constant maintenance. The bimodal tendency of damage repartition could also suggest the presence of buildings with different vulnerability, belonging to the same building typology, which is indeed defined by pooling together constructions with similar structural characteristics. Nevertheless, vulnerability factors and structural/architectural features, which are not contemplated by either the survey form (e.g. distribution of walls and openings, architectural configuration, construction details) or the adopted taxonomy (e.g. plan and elevation irregularities), may imply heterogeneity within the same typology. The peculiar damage repartition could be also affected by several uncertainties associated with the seismic input characterisation, such as the poor correlation between the peak ground acceleration and the observed seismic damage, a coarse seismic input definition (at the municipality level) and the use of ground motion prediction equations to estimate the preselected ground motion intensity measure.

Starting from these considerations, different approaches were considered for the interpretation and prediction of observed damages. The limitations of the classical binomial model for reproducing the subdivision of damage in the different levels were overcome by proposing two hybrid methodologies. The first imposes the binomial model only on the higher levels of damage (DS2–DS5), but it does not allow distinguishing buildings with either slight or null damage, which do not follow the binomial model. The information

on buildings binomially and non-binomially distributed is then combined, to derive a continuous description of the seismic vulnerability as a function of PGA. The second approach predicts the probability of occurrence of the different damage states by simultaneously considering two binomial distributions, capturing the trend of the lower and higher damage levels, respectively.

The different models were applied to all considered building typologies and their error in fitting the observed damage data was evaluated by means of a synthetic parameter. For each typology, the approach providing the best fit to the empirical data was identified and the parameters required for its application are reported at the end of the paper, together with the corresponding damage probability matrices. This allows the application of the proposed approaches for forecasting the distribution of the expected damage, for a given building typology and a given ground motion level (expressed in terms of PGA on rock). Although the parameters have been calibrated on damage data from a specific event occurred in a precise region of Italy, it is believed that the results could be applied elsewhere, provided the seismic hazard and the construction typologies are similar to the Italian context.

References

Akkar S, Sandıkkaya MA, Senyurt M, Sisi AA, Ay BÖ, Traversa P, Douglas J, Cotton F, Luzi L, Hernandez B, Godey S (2014) Reference database for seismic ground motion in Europe (RESORCE). Bull Earthq Eng 12(1):311–339

Anagnostopoulos S, Moretti M (2008) Post-earthquake emergency assessment of building damage, safety and usability—Part 1: technical issues. Soil Dyn Earthq Eng 28(3):223–232

Angeletti P, Baratta A, Bernardini A, Cecotti C, Cherubini A, Colozza R, Decanini L, Diotallevi P, Di Pasquale G, Dolce M, Goretti A, Lucantoni A, Martinelli A, Molin D, Orsini G, Papa F, Petrini V, Riuscetti M, Zuccaro G (2002) Valutazione e riduzione della vulnerabilità sismica degli edifici, con particolare riferimento a quelli strategici per la protezione civile. Rapporto finale della commissione tecnico-scientifica per l'aggiornamento dell'inventario e della vulnerabilità degli edifici residenziali e pubblici per la stesura di un glossario **(in Italian)**

ATC, Applied Technology Council (2005) Field manual post-earthquake safety evaluation of buildings (ATC-20-1), 2nd edn. ATC, Applied Technology Council, Redwood City

Augenti N, Parisi F (2010) Learning from Construction Failures due to the 2009 L'Aquila, Italy, earthquake. J Perform Constr Facil 24(6):536–555

Baggio C, Bernardini A, Colozza R, Corazza L, Della Bella M, Di Pasquale G, Dolce M, Goretti A, Martinelli A, Orsini G, Papa F, Zuccaro G (2007) Field manual for post-earthquake damage and safety assessment and short-term countermeasures (AeDES). Translation from Italian: Rota M., Goretti A. JRC Scientific and Technical Reports, EUR 22868 EN-2007

Bindi D, Massa M, Luzi L, Ameri G, Pacor F, Puglia R, Augliera P (2014a) Pan-European ground-motion prediction equations for the average horizontal component of PGA, PGV and 5%-damped PSA at spectral periods up to 3.0 s using the RESORCE dataset. Bull Earthq Eng 12(1):391–430

Bindi D, Massa M, Luzi L, Ameri G, Pacor F, Puglia R, Augliera P (2014b) Erratum to: Pan-European ground-motion prediction equations for the average horizontal component of PGA, PGV and 5%-damped PSA at spectral periods up to 3.0 s using the RESORCE dataset. Bull Earthq Eng 12(1):431–448

Braga F, Dolce M, Liberatore D (1982) A statistical study on damaged buildings and an ensuing review of the M.S.K.-76 scale. In: Proceedings of the 7th European conference on earthquake engineering, Athens

Braga F, Manfredi V, Masi A, Salvatori A, Vona M (2011) Performance of non-structural elements in RC buildings during the L'Aquila, 2009 earthquake. Bull Earthq Eng 9(1):307–324

Buratti N, Minghini F, Ongaretto E, Savoia M, Tullini N (2017) Empirical seismic fragility for the precast RC industrial buildings damaged by the 2012 Emilia (Italy) earthquakes. Earthq Eng Struct D 46(14):2317–2335

Carocci CF, Lagomarsino S (2009) Gli edifici in muratura nei centri storici dell'Aquilano, Progettazione Sismica, vol 3. IUSS Press, Pavia, pp 117–131 **(in Italian)**

Census Data (2001) http://dawinci.istat.it/jsp/MD/dawinciMD.jsp

D'Ayala D, Dolce M (2011) Guest editorial: L'Aquila earthquake: seismic sequence of the 6th April 2009, Abruzzo, Italy. Bull Earthq Eng 9(1):1–10

D'Ayala D, Paganoni S (2011) Assessment and analysis of damage in L'Aquila historic city centre after 6th April 2009. Bull Earthq Eng 9(1):81–104

De Luca F, Verderame GM, Manfredi G (2015) Analytical versus observational fragilities: the case of Pettino (L'Aquila) damage data database. Bull Earthq Eng 13(4):1161–1181

Del Gaudio C, De Martino G, Di Ludovico M, Manfredi G, Prota A, Ricci P, Verderame GM (2017) Empirical fragility curves from damage data on RC buildings after the 2009 L'Aquila earthquake. Bull Earthq Eng 15(4):1425–1450

Di Ludovico M, Prota A, Moroni C, Manfredi G, Dolce M (2017) Reconstruction process of damaged residential buildings outside historical centres after the L'Aquila earthquake: part I—"light damage" reconstruction. Bull Earthq Eng 15(2):667–692

Di Pasquale G, Goretti A (2001) Functional and economic vulnerability of residential buildings affected by recent Italian earthquakes. In: Proceedings of the 10th national conference of seismic engineering in Italy, Potenza-Matera, Italy **(in Italian)**

Di Pasquale G, Orsini G (1997) Proposta per la valutazione di scenari di danno conseguenti ad un evento sismico a partire dai dati ISTAT. In: Proceedings of the 8th Italian conference on earthquake engineering, Taormina, Italy **(in Italian)**

Dolce M, Di Bucci D (2014) National Civil Protection Organization and technical activities in the 2012 Emilia earthquakes (Italy). Bull Earthq Eng 12(5):2231–2253

Dolce M, Goretti A (2015) Building damage assessment after the 2009 Abruzzi earthquake. Bull Earthq Eng 13(8):2241–2264

Filiatrault A, Sullivan T (2014) Performance-based seismic design of nonstructural building components: the next frontier of earthquake engineering. Earthq Eng Eng Vib 13:17–46

Galli P, Camassi R, Azzaro R, Bernardini F, Castenetto S, Molin D, Peronace E, Rossi A, Vecchi M, Tertulliani A (2009) April 6, 2009 L'Aquila earthquake: macroseismic survey, surficial effects and seismotectonic implications. Ital J Quat Sci 22(2):235–246

Goretti A, Di Pasquale G (2004) Building inspection and damage data for the 2002 Molise, Italy, earthquake. Earthq Spectra 20(S1):S167–S190

Grünthal G (ed.) Musson RMW, Schwarz J, Stucchi M (1998) European Macroseismic Scale. Cahiers du Centre Européen de Géodynamique et de Séismologie, vol 15, Luxembourg

Hancilar U, Taucer F, Corbane C (2013) Empirical fragility functions based on remote sensing and field data after the 12 January 2010 Haiti earthquake. Earthq Spectra 29(4):1275–1310

Hsieh MH, Lee BJ, Lei TC, Lin JY (2013) Development of medium- and low-rise reinforced concrete building fragility curves based on Chi-Chi earthquake data. Nat Hazards 69:695–728

Ioannou I, Douglas J, Rossetto T (2015) Assessing the impact of ground-motion variability and uncertainty on empirical fragility curves. Soil Dyn Earthq Eng 69:83–92

JBDPA, The Japan Building Disaster Prevention Association, JBDPA (1991) Guideline for post-earthquake damage evaluation and rehabilitation (revised in 2001)

Kouris L (2016) Seismic fragility curves for timber-framed masonry structures based on empirical damage data. IJSMSS 2(Nos. 3/4):233–249

Lagomarsino S, Giovinazzi S (2006) Macroseismic and mechanical models for the vulnerability and damage assessment of current buildings. Bull Earthq Eng 4:415–443

Lagomarsino S, Cattari S, Ottonelli D (2015) Derivazione di curve di fragilità empiriche per classi tipologiche rappresentative del costruito Aquilano sulla base dei dati del danno dell'evento sismico del 2009. Research Project DPC-ReLUIS 2015

Liel AB, Lynch KP (2009) Vulnerability of reinforced concrete frame buildings and their occupants in the 2009 L'Aquila, Italy earthquake. Quick Response Report

Maffei J, Bazzurro P, Marrow J, Goretti A (2006) Recent Italian earthquakes: examination of structural vulnerability, damage, and post-earthquake practices. Earthquake Engineering Research Institute Report, Oakland. ISBN 1-932884-12-2

Miranda E, Mosqueda G, Retamales R, Pekcan G (2012) Performance of nonstructural components during the 27 February 2010 Chile earthquake. Earthq Spectra 28(S1):S453–S471

Molina S, Torres Y, Benito B, Navarro M, Belizaire D (2014) Using the damage from the 2010 Haiti earthquake for calibrating vulnerability models of typical structures in Port-au-Prince (Haiti). Bull Earthq Eng 12(4):1459–1478

NZSEE, New Zealand Society for Earthquake Engineering (2011) Building safety evaluation following the Canterbury earthquakes, Report to the royal commission of inquiry into building failure caused by the Canterbury earthquakes, September, Wellington, New Zealand

Penna A, Morandi P, Rota M, Manzini CF, Da Porto F, Magenes G (2014) Performance of masonry buildings during the Emilia 2012 earthquake. Bull Earthq Eng 12(5):2255–2273

Pomonis A, Gaspari M, Karababa FS (2014) Seismic vulnerability assessment for buildings in Greece based on observed damage data sets. Boll Geofis Teor Appl 55(2):501–534

Ricci P, De Luca F, Verderame GM (2011) 6th April 2009 L'Aquila earthquake, Italy: reinforced concrete building performance. Bull Earthq Eng 9(1):285–305

RISK-UE (2004) The European Risk-UE Project: An advanced approach to earthquake risk scenarios. www.risk-ue.net

Roca A, Goula X, Susagna T, Chavez J, Gonzalez M, Reinoso E (2006) A simplified method for vulnerability assessment of dwelling buildings and estimation of damage scenarios in Catalonia, Spain. Bull Earthq Eng 4(2):141–158

Rossetto T, Elnashai A (2003) Derivation of vulnerability functions for European-type RC structures based on observational data. Eng Struct 25(10):1241–1263

Rossetto T, Peiris N, Alarcon JE, So E, Sargeant S, Free M, Sword-Daniels V, Del Re D, Libberton C, Verrucci E, Sammonds P, Faure Walker J (2011) Field observations from the Aquila, Italy earthquake of April 6, 2009. Bull Earthq Eng 9(1):11–37

Rossetto T, Ioannou I, Grant DN (2013) Existing empirical vulnerability and fragility functions: Compendium and guide for selection. GEM Technical Report 2013-X, GEM Foundation, Pavia, Italy

Rosti A, Rota M (2017) Comparison of PSH results with historical macroseismic observations at different scales. Part 2: application to South-East France. Bull Earthq Eng 15(11):4609–4633

Rota M, Rosti A (2017) Comparison of PSH results with historical macroseismic observations at different scales. Part 1: methodology. Bull Earthq Eng 15(11):4585–4607

Rota M, Penna A, Strobbia C (2008) Processing Italian damage data to derive typological fragility curves. Soil Dyn Earthq Eng 28(10–11):933–947

Rota M, Penna A, Strobbia C, Magenes G (2011) Typological seismic risk maps for Italy. Earthq Spectra 27(3):907–926

Saatcioglu M, Bruneau M (1993) Performance of structures during 1992 Erzincan earthquake. Can J Civil Eng 20:305–325

Sabetta F, Goretti A, Lucantoni A (1998) Empirical fragility curves from damage surveys and estimated strong ground motion. In: Proceedings of the 11th European conference on earthquake engineering, Balkema, Rotterdam

Sorrentino L, Liberatore L, Liberatore D, Masiani R (2014) The behaviour of vernacular buildings in the 2012 Emilia earthquakes. Bull Earthq Eng 12(5):2367–2382

Stucchi M, Meletti C, Rovida A, D'Amico V, Gomez Capera AA (2009) Terremoti storici e pericolosità sismica dell'area aquilana. Progettazione Sismica 3:23–34 **(in Italian)**

Studer JA, Jordi M, Lateltin O, Werner C (2010) Manuale per la valutazione degli edifici dopo un terremoto. Ufficio federale della protezione della popolazione UFPP, Associazione degli istituti cantonali di assicurazione antincendio AICAA e Associazione svizzera d'assicurazioni ASA (ed.), Bern, Switzerland

Vicente RS, Rodrigues H, Varum H, Costa A, Mendes da Silva JAR (2012) Performance of masonry enclosure walls: lessons learned from recent earthquakes. Earthq Eng Eng Vib 11(1):23–34

Yazgan U (2015) Empirical seismic fragility assessment with explicit modelling of spatial ground motion variability. Eng Struct 100:479–489

Zucconi M, Sorrentino L, Ferlito R (2017) Principal component analysis for a seismic usability model of unreinforced masonry buildings. Soil Dyn Earthq Eng 96:64–75